-

The building of an accurate 3D physical model of the skull and maxillary dentition.

By

Michael O'Neil

Thesis submitted in fulfilment of the requirements for the degree of Master of Medical Science (MSc)

Faculty of Medicine
University of Glasgow
June 2010

Contents

Abstract

3D rapid prototyping is a useful tool for the production of 3D models of the human skull taken from cone beam computed tomography scans. Although the accuracy of these models is acceptable the dentition is distorted. The aim of the study is to replace the inaccurately reproduced dental arch of a 3D printed skull model with accurate, correctly proportioned plaster teeth, obtained from a dental impression.

6 dried human skulls were scanned using a Faro laser arm scanner. Impressions of the dentition were taken using silicone impression material. Plaster dental casts were produced using dental stone. Following removal of the inaccurate dentition from the 3D printed skull model, the corresponding plaster dental cast was attached to the 3D printed skull model using a custom designed technique. The six modified 3D printed skull models with replaced dentition were laser scanned using a Faro arm. VRmesh software was used to superimpose the laser scanned skull images.

List of Charts:

Chapter 3.

Chapter 5.

List of Tables:

Chapter 3.

Chapter 4.

Chapter 5.

List of Figures:

Chapter 2.

Chapter 3.

Chapter 4.

Chapter 5.

Chapter 6.

PREFACE

This study was carried out at the University of Glasgow Dental Hospital and School. The laboratory experiments were performed at the West of Scotland Regional Maxillofacial Prosthetics Laboratory at the Southern General Hospital Glasgow. The study was carried out under the supervision of Professor A. Ayoub, Dr B. Khambay, Mr F.S. Walker, Professor K.F. Moos O.B.E. and Professor J.C. Barbenel.

This thesis represents the original work carried out by the author and has not been submitted in any form to any other university.

ACKNOWLEDGMENTS

I would like to sincerely thank Professor A.F. Ayoub for having faith and trust in my technical abilities to achieve the aims of this project. I also would like to thank him for giving me this prestigious opportunity to study at a level that I had never imagined I was capable of and to be associated with the world famous university in the city I was born. I am forever in your debit.

To Professor K.F. Moos O.B.E. for his wealth of experience, support, guidance and encouragement that has been called upon many times in this study.

To Professor J.C. Barbenel for his depth of knowledge, his support and encouragement in making sure the project maintained focus on what was trying to be achieved.

To Dr B Khambay for his endless help and assistance using the computer software necessary for this project to be completed.

To Mr. F.S. Walker, for being a true and dependable friend and allowing me the pleasure of working with him. For his unconditional loyalty and trust in my ability to cope with the problems this project would provide.

To Professor A. Bowman my most heartfelt thanks for all his help with the statistical analysis of this project.

To Alison McCormack for all her help, encouragement and assistance during the course of this study.

My thanks to the Stephen Plumpton Fund, The Scottish Association for Cleft Lip and Palate and the NHS bursary scheme for financially contributing to this project.

To the Medical Illustration department at the Southern General Hospital Glasgow, with a special thanks to James Eyland for all his highly specialist expertise in providing the fantastic illustrations for this project.

Last of all I would like to sincerely thank my wife and family, their support and encouragement over the years has been enormous. To my wife I would like to thank her for teaching me how to study, I could never have achieved what I have without her. It is to my wife and family I dedicate this thesis.

"Pain is temporary. It may last a minute, or an hour, or a day, or a year, but eventually it will subside and something else will take its place. If I quit, however, it lasts forever."
Lance Armstrong.

In recent years it has been encouraging to witness the positive signs of a worldwide growth in solidarity towards the poor. But to turn this solidarity into effective action calls for fresh thinking that will improve life conditions in many important areas, such as food production, clean water, job creation, education, support to families, especially migrants, and basic healthcare. Where human lives are concerned, time is always short: yet the world has witnessed the vast resources that governments can draw upon to rescue financial

institutions deemed “too big to fail”. Surely the integral human development of the world’s peoples is no less important: here is an enterprise, worthy of the world’s attention, that is truly “too big to fail”.

Pope Benedict's address to Politicians, Diplomats, Academics and Business Leaders. September 17 2010.

DECLARATION

This thesis represents the original work of the author.

Michael O'Neil

June 2010

1

INTRODUCTION

1.1 Introduction

Orthognathic surgery planning has been routinely carried out on various types of dental articulators. From a simple hinge articulator where a straightforward single jaw movement is required with no vertical height change, to a more complicated bi-maxillary procedure which involves altering both jaws. Bi-maxillary planning procedures are carried out using a semi adjustable articulator and its corresponding facebow. These procedures can involve maxillary impaction or down grafting, together with advancement or retraction of the mandible in order to achieve best occlusion and correction of facial deformity. A facebow registration is used to transfer the patients' maxillary occlusal plane to the semi adjustable articulator. However, there are inaccuracies when planning orthognathic surgery prediction on semi adjustable articulators. Semi adjustable articulators are primarily used for making dentures for which they are suitable and if the maxillary occlusal plane is altered, as the teeth are being placed in modelling wax, this does not affect the function of the denture constructed. However, it is documented by Walker *et al* (2008) that if the maxillary occlusal plane is altered during orthognathic surgery planning cases, then this has a signification effect on the outcome for the patient. Walker *et al* (2008) also highlighted the importance of accurately recording the maxillary occlusal plane in relation to the base of the skull for orthognathic planning. He stated that it is in this area that most inaccuracies occur when using semi adjustable articulator systems for orthognathic surgery prediction.

It is my aim to investigate the use of 3Dimentional (3D) printed skull models in the search for a more accurate process for carrying out orthognathic surgery prediction. However, at present there are some drawbacks to using 3D printed skull models for orthognathic predicted surgery. Inaccurate reproduction of the occlusal planes of the teeth is due to CT

scans being influenced by metallic dental restorations that cause various artefacts. In addition, the teeth themselves do not replicate accurately due to their enamel and dentine composition.

My goal is to find a way of replacing the inaccurate dentition on the 3D printed skull model with plaster casts of the patients' dentition. This process will require the plaster casts to be accurately placed into position to emulate the same anatomical position as the patients' natural dentition. If this can be achieved, it will allow surgeons and technologists to see increased anatomical structure and allow accurate estimation of impaction, using anatomical points of reference. Surgeons will be able to visualise and measure autorotation of the mandible and adapt bone plates and fixing devices prior to surgery. A further benefit of the 3D printed skull models is that they provide an accurate indication of size when a bone graft is required. Irrespective of the quality of 3D visual models on a computer screen surgeons still favour hands on models to plan and simulate procedures pre-operatively. In conclusion, having a 3D printed skull model of the patient allows the surgeon many more advantages than are available at present.

2

Background of the limitations of facebow and articulator systems for orthognathic model surgery.

2.1 Background

Orthognathic surgery planning is a method used by surgeons to plan the repositioning of patients with skeletal jaw deformities. Facial deformity can vary from patient to patient. Some can be complex congenital deformities that the patient has had since birth, where part of their skeletal shape has not developed properly prior to being born. Others are dento-facial, which tend to develop as the patient grows into adulthood and the skeletal relationship changes. Patients with skeletal problems would normally be referred by a doctor or dentist to a specialist clinic to be diagnosed and treated for their condition. This would very often involve an operation in order to improve their skeletal relationship. The patient would have photographs, X-rays, dental impressions and a wax wafer occlusal bite of their dentition taken in order to develop a treatment plan for the correction of the skeletal deformity. The dental impressions are cast in plaster to give an exact copy of the patients' dental relationship. These plaster casts are then mounted on an apparatus which artificially simulates the patients' jaw relationship. The apparatus commonly used for planning the correction of these procedures is a Dental Articulator. The plaster models of the patient's dental arches are attached to the articulator and occluded using a wax wafer bite registration taken from the patient.

2.2 Articulators

There are various dental articulators that can be used for this process. Much depends on the specific nature of the patients' deformity. If a patient requires a single jaw procedure, either a set back or advancement to the maxilla or mandible, where there is no change to the facial height of the patient i.e. the patient's face will not be made longer or shorter, then a simple hinge articulator is used. *(Figure.2.1)* A simple hinge articulator is a basic but useful style of articulator for this purpose.

Figure.2.1 Simple hinge articulator.

If the facial height has to be altered or the maxilla and mandible are being repositioned then a semi-adjustable articulator and its corresponding facebow are utilised. *(Figure.2.2), (Figure.2.3)*

Figure.2.2 Semi-adjustable articulator.

.

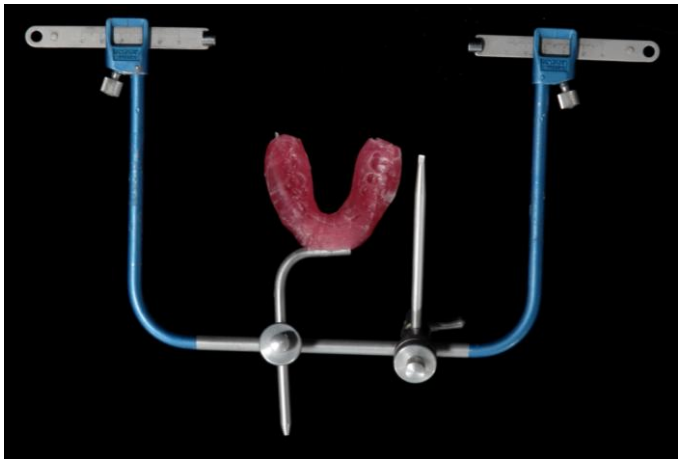

Figure.2.3 The facebow.

This particular type of articulator involves recording anatomical reference points of the patient, e.g. auditory meatus, nasion, condyles, orbitale and the maxillary occlusal plane of

the dentition. A facebow is used for this purpose and the reference points are recorded by devices attached to the facebow. The facebow is then attached to the semi-adjustable articulator. A maxillary plaster cast, made from impressions taken of the patients' dentition, is then mounted onto the semi-adjustable articulator using the reference points taken by the facebow to replicating the position of the natural maxilla. The mandibular cast is attached onto the semi-adjustable articulator using the wax bite record of the patient in occlusion. It should be noted that there are different types of facebow and articulator systems that can be used to record the maxillary position and some are more accurate than others. However, all articulators have varying degrees of inaccuracy owing to the fact that facebows are average value. This means for patients with non-average facial settings, including the majority of orthognathic surgery patients, semi-adjustable articulators are not suitable. These findings have been well documented in the literature. Walker *et al* (2008) has provided a new facebow *(Figure.2.4)* and orthognathic articulator *(Figure.2.5)* which greatly reduces the inaccuracy of transferring the position of the natural maxilla onto an articulator.

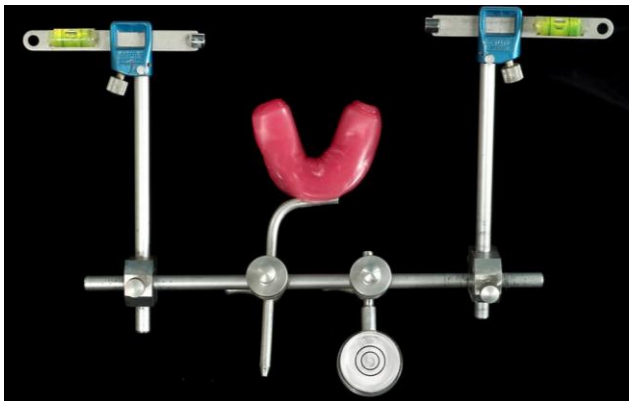

Figure.2.4 The new Orthognathic facebow.

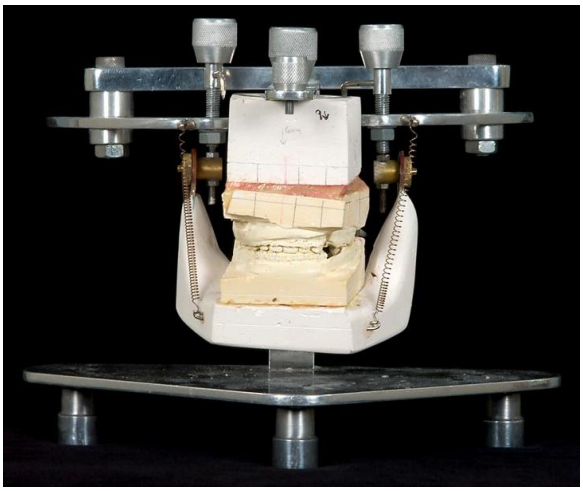

Figure.2.5 The Orthognathic articulator.

This concept works by adjusting the arms of the orthognathic articulator to accommodate the orthognathic facebow. With other facebows and semi-adjustable articulators the opposite occurs and the facebows are designed to fit the articulators. Walkers' system also takes into account patients with asymmetry problems by using anatomical references indicators which can be adjusted to replicate the patient's dental facial condition. Whilst Walker (2008) has greatly improved levels of accuracy for transferring the position of the maxillary cast to an articulator, there are still inaccuracy problems in this new technique due to soft tissue coverage of reference areas.

2.3 Orthognathic planning procedure

Once the models are articulated the surgeon supplies a prediction sheet indicating what will be required and a record of anatomical areas is also made - namely the patients chin point, the centre lines of the teeth and any asymmetry of the face or mandible. Cephalometric analysis *(Figure.2.6)* of the patient is carried out by the surgeon. This is done by cutting and sectioning X-rays and repositioning them to give the best possible skeletal profile for the patient.

Figure.2.6 Cephalograph.

There are computer software packages that can carry out this prediction and calculate the movements involved. These, together with the articulated dental casts help to plan for the best predicted outcome for the patient. In order to replicate the patients' current dental relationship the dental casts are attached to the articulator using dental plaster and reference points are marked onto the articulating plaster. The maxillary cast is then detached and moved into its predicted position before being reattached to the articulating plaster using modelling wax. Comparing the original reference marks on the articulating plaster with the final placement of the maxilla provides a plan of the movements which will be required in theatre. In the same way the mandibular cast is moved to line up with the maxillary cast to achieve the best occlusion before being reattached to the articulating plaster. A registration of this new relationship of the maxilla to mandible is taken at incisal and cusp level using a clear self-curing acrylic resin *(Figure.2.7).* This registration is the template the surgeon will use to reposition the patients' new skeletal relationship in theatre. Prior to fitting the final clear acrylic wafer, the surgeon must firstly move the maxilla; to do this an intermediate wafer is required. This is made in a different coloured self curing acrylic resin to distinguish it from the final inter-occlusal wafer.

Figure.2.7 Inter-Occlusal wafers, final (left) and intermediate (right).

In order to make the intermediate wafer the mandibular cast is moved back to the original position and reattached to the articulating plaster. The maxillary plaster cast remains in its new final position and the coloured self curing acrylic wafer is made by rotating the mandible to occlude with the maxilla. This coloured wafer is the template the surgeon will use to reposition the patient's maxilla. It should be made clear that when simulating the new skeletal position on the articulator, the final skeletal position is recorded first and the clear self cure acrylic wafer made; this is done so that there is no damage to the incisal and occlusal areas of the model. Then the intermediate position is simulated on the articulator and the coloured intermediate wafer is constructed. The opposite happens in theatre, the intermediate position is achieved first, then the final position. Once the patients' maxilla is moved into its new position, it is secured using bone plates and screws. The patients' mandible is then sectioned and moved into line with the final clear self cure acrylic wafer and is fixed using bone plates and screws. The patients' dentition is held together in this wafer in order to hold the new skeletal position.

2.4 3Dimentional printed skull models

With the introduction of Rapid Prototyping (R.P.) from digital images, medical anatomical models are being used more and more as an aid for surgical planning. They allow preoperative simulation for surgeons via virtual images on the screen and in the form of 3D

printed skull models. The information taken from Cone Beam Computed Tomography (CBCT), Magnetic Resonance Imaging (MRI) and Ultra Sound scans allows the production of 3D skull models using 3D rapid printing machines. *(Figure.2.8)*

Figure.2.8 Rapid prototype 3D printer.

For orthognathic surgery planning these 3D printed skull models are of great value as they allow the surgeon to see all the anatomical areas and provide a greater understanding of what to expect when in theatre. In addition, the 3D printed models *(Figure2.9)* allow for preoperative contouring of bone plates, indicate the size of bone graft which will be required and display what will happen should the mandible auto-rotate.

Figure.2.9 3D model made from volumetric CT image data.

At present the surgeon has lateral cephalographs, X-rays and dental casts of the dentition and alveolar areas on which to plan their surgery. The inclusion of this new level of

technology would greatly enhance and improve planning, save on theatre time and help to explain the procedure to patients. Another added feature is their use as a teaching aid.

At present, a 3D printed skull model replicates well, the hard tissue areas of the skull due to the bone density being captured in the CT scanned image. The same cannot be said for the dentition which is made up of different tissue to bone. The dentition produces various inaccuracies due to its enamel and dentine composition, dental restorations and orthodontic attachments. These errors are consistent when using either a multi-slice CT or CBCT scanner. CBCT scanning is recommended for orthognathic planning, due to the fact that it exposes the patient to lower levels of radiation, Swennen *et al* (2007). In this study it is my aim to create a 3D printed skull model from a CBCT scan and successfully remove the inaccurate dentition, replacing it with a maxillary dental casts made from impressions taken directly from the natural teeth. If successful the adapted 3D printed skull model would allow surgeons preoperative simulation and planning opportunities but with the added advantage of having dimensionally accurate dentition. It is hoped that with the new dentition in position, orthognathic surgery planning could be carried out using 3D printed skull models rather than by using facebows and dental articulators with their limitations and inaccuracies.

3

Literature Review

There is a considerable array of literature available which offer opinions on the use of articulators and facebow systems for Orthognathic model surgery planning. Orthognathic model surgery planning is routinely carried out on semi-adjustable articulators; the maxillary dental arch is transferred to the articulator using a facebow registration of anatomical points on the patient's face. The facebow recording relates the maxillary cast to the upper arm of the semi-adjustable articulator using three points of reference, the condyles or the auditory meateae, the maxillary occlusal plane and orbitale. These recordings were assumed to reproduce the patients' maxillary relationship with the mandibular condyles. Ellis *et al* (1992) and Gateno *et al* (2001) both point out that semi adjustable articulators were never designed for use in Orthognathic model surgery planning. They both recognised that the upper arm of the semi-adjustable articulator is universally accepted to replicate the Frankfort horizontal plane. However, Gateno indicated that when taking a facebow recording the condylar rods were aligned to the centre of the condyle and the orbital pointer was aligned to orbitale, those points recorded a plane known as the axis-orbital plane which was approximately 13 degrees steeper than the Frankfort horizontal plane. Therefore there was a disparity between the planes which introduced an error when mounting the maxillary cast onto the semi-adjustable articulator.

3.1 Facebow registration

Ferrario *et al* (2002) had similar findings when he assessed the reliability of facebow transfer. Ellis *et al* (1992) carried out a study on the accuracy of facebow transfer on 25 patients using a Hanau facebow and semi-adjustable articulator. The aim was to test the accuracy of transferring the facebow recordings from the patients onto the semi-adjustable articulators and compare the mounted maxillary casts with the planes identified on the cephalograms with particular attention being given to the maxillary occlusal plane angle. If

the maxillary occlusal plane angle is not replicated accurately on the semi-adjustable articulator then any subsequent model planning carried out on the mounted casts would be incorrect and would produce an inexact inter-occlusal wafer position, therefore affecting the final outcome in the operating theatre. The results of the study showed that the maxillary occlusal plane angle differed by 7 degrees on average from that identified from the cephalogram. With the exception of two cases, the maxillary occlusal plane angle was steeper on the semi-adjustable articulator than that taken from the cephalogram. Ellis *et al* (1992) stated, that in order to correct this inaccuracy, the maxillary occlusal plane angle should be observed when the maxillary cast was on the bite fork prior to it being attached to the semi-adjustable articulator. If the maxillary occlusal plane angle was different to that taken from the cephalogram, the facebow should be rotated up or down until the maxillary occlusal plane angle was similar to the cephalogram prior to mounting the cast onto the semi-adjustable articulator.

Gonzalez and Kingery (1968) detected errors in facebow transfer. A study was carried out on 21 patients, cephalograms and facebows were taken and used to measure 3 different planes of reference which were then measured against the Frankfort horizontal plane, the maxillary ridge plane, the occlusal plane and the axis orbital plane. The results indicated that none of the true planes were maintained when the maxillary cast was transferred to the semi-adjustable articulator. However, the axis orbital plane had the least amount of error with the maxillary occlusal plane having the worst. Semi-adjustable articulators have been engineered with the upper horizontal arm representing the Frankfort horizontal plane, however, not every patient has a horizontal Frankfort plane as highlighted by Downs (1956) *(Figure.3.1)* Therefore inaccuracies will be a common issue when using the currently available facebows and semi-adjustable articulators.

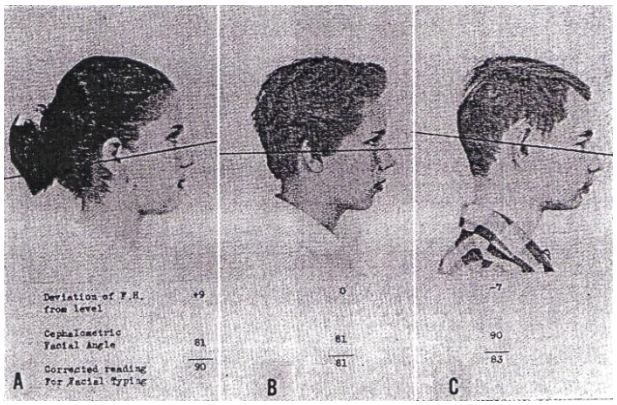

Figure.3.1 Variations of Frankfort Horizontal plane. Discrepancies highlighted by Downs (1956).

3.2 Potential solutions to facebow inaccuracy

Gonzalez and Kingery (1968) recommended that a compensation for this error could be achieved in one of two ways. The orbital pointer could be placed 7mm below orbitale during the facebow registration or the orbital pointer be placed 7mm above the orbital indicator of the semi-adjustable articulator when mounting the casts. The latter method was suggested also by Stade *et al* (1982). Gonzalez and Kingery (1968) pointed out that this would put the arbitrary condylar axis point and the orbital pin on approximately the same level as a horizontal plane. This reference would then be transferred from the patient to the semi-adjustable articulator providing a more reliable reference transfer, as the orbital indicator and the condylar axis were then related to a horizontal plane on the semi-adjustable articulator, providing improved accuracy for the transfer of the maxillary cast. It has been emphasised that the effect of a 7mm shift of the orbital pointer was still an unknown factor and the figure was an average and if greater accuracy was needed then an actual measurement of the distance of the condylar axis point to the Frankfort horizontal plane should be used. Pitchford *et al* (1991) and Bailey and Nowlin (1984) suggested that the orbital pin height be increased to 18mm and 16mm above the orbital indicator. Interestingly it appeared that there was some debate between authors as to how much

compensation should be carried out prior to the mounting of the maxillary cast onto the semi-adjustable articulator. However, they were unanimous that there was an error when transferring the facebow to the semi-adjustable articulator.

Sharifi *et al* (2008) stated in such cases where there was a discrepancy between the maxillary occlusal plane angle on the cast and the upper arm of the semi-adjustable articulator this would result in inaccuracies between the patients' maxillary occlusal plane angle and the Frankfort horizontal plane. Sharifi *et al* recognised that this could cause problems when impacting the maxilla in model surgery. This would lead to a false prediction and depending on the difference in the maxillary occlusal angle, would require a greater degree of maxillary impaction than was predicted on the semi-adjustable articulator. It has been pointed out that it would be good practice to check with the lateral cephalogram as to the accuracy of the maxillary occlusal plane when mounting the cast onto the semi-adjustable articulator, a method described also by Ellis *et al* (1992).

3.3 Orthognathic surgery planning systems

Bamber *et al* (2001) carried out a validation of the two most popular orthognathic model surgery techniques in the United Kingdom, the Lockwood keyspacer technique *(Figure. 3.2)* and the Eastman anatomically oriented technique *(Figure.3.3)*.

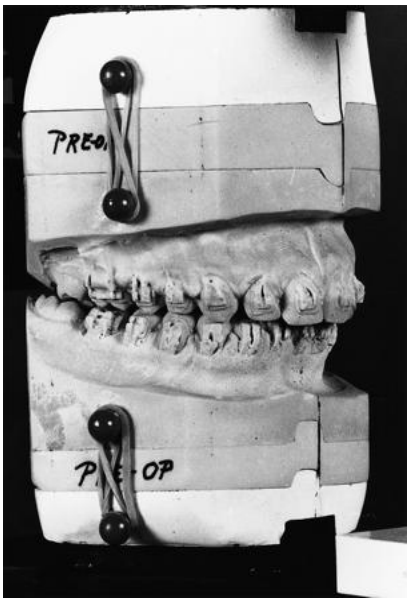

Figure.3.2 Lockwood Technique.

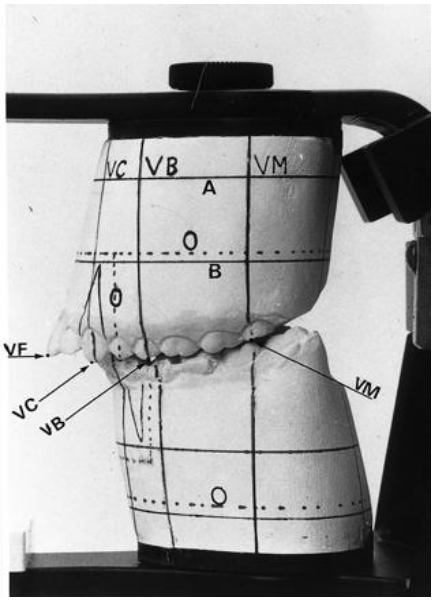

Figure.3.3 Eastman Technique.

The Lockwood keyspacer technique involves inserting a thin layer of plaster or a plastic keyspacer between upper and lower models; they are usually 7mm in thickness and shaped to the angle of the trimmed dental model base. The spacers are held in place using elastics, plastic locks and in some cases magnets. This technique was first used on simple hinge articulators; however, the system has been enhanced with the use of facebow registration and anatomical articulators.

The Eastman anatomically orientated model surgery technique uses a facebow recording taken in a supine centric relationship. This involves the patient lying flat on their back with their face upwards. The facebow position is transferred onto the semi adjustable articulator and then the models are articulated. Horizontal and vertical lines are drawn on the mounting plaster to register the pre-operative positions of the maxilla and mandible.

The purpose of this study was to determine the accuracy of the positioning of the maxillary cast in relation to a prescribed treatment plan. The results found that the Lockwood keyspacer technique disadvantaged patients with a steep occlusal-Frankfort plane angle

who required a large vertical impaction. This was due to the keyspacer mounting plaster being too thick (7mm). When a large impaction was required the keyspacer mounting plaster would be rendered inadequate which would then require the maxillary model to be trimmed. This would affect the thickness of the cast and would also result in the angles parallel sides being lost. The angles parallel sides are ideal for detecting any unwanted rotation of the maxillary cast. The Eastman technique does not have angle trimmed edges therefore was in danger of 'building in' unwanted rotations. The Eastman technique uses wax to hold the post-operative position which could contract on cooling again altering the position of the plaster segments allowing dimensional inaccuracy to occur. Bamber *et al* (2001) concluded that both surgery planning systems failed to carry out the prescribed treatment plans accurately. However the statistical report showed the errors in the Lockwood technique to be higher in the vertical and anterior-posterior planes than the Eastman technique, but Lockwood was better in the medio-lateral plane.

3.4 Orthognathic articulators and facebows

It would appear that inaccuracies were evident when using a facebow and a semi-adjustable articulator system for Orthognathic prediction surgery. The need for an improvement in accuracy of facebow transfer, better designed articulators for orthognathic model surgery planning purposes and the use of 3D skull models would seem to hold the key to a more accurate prediction for Orthognathic planning. Walker *et al* (2008), Sharifi *et al* (2008), Ellis *et al* (1992), Pitchford *et al* (1991), Bailey and Nowlin (1984), Stade *et al* (1982) and Gonzalez and Kingery (1968) have all recognised inaccuracy occurring during transfer of the maxillary model with the facebow at a fixed maxillary occlusal plane angle. Walker *et al* (2008) emphasised the importance of having the maxillary cast accurately mounted on the semi adjustable articulator, similar to the patients' maxilla relative to the base of the skull. The reason for this required accuracy was to enhance the precision of the

model surgery planning. Walkers' facebow technique involved recording the patient natural head posture using a facebow with a spirit level attached, instead of with an orbital pointer. This worked by having the patient sitting upright in a chair two metres away from a full length mirror. A line three millimetres thick runs vertically down the mirrors full length. The patients are instructed to look into their own eyes in the mirror, making sure the vertical line on the mirror is centred on the reflected image. This is consistent with the system Moorrees and Keen adopted for measuring the natural head position, (1958).

Walker compared his new facebow technique with the conventional methods of facebow recording. Six patients were recruited, lateral cephalograms were taken as well as two facebow recordings, one using the condyles and an orbital pointer to record left orbitale, the other method used the condyles and a spirit level to record the natural head position in a horizontal plane. All casts were mounted on a semi-adjustable articulator. A flat plate was placed across the maxillary occlusal plane of each mounted cast and the angle measured with a protractor. The results were compared to lateral cephalograms to check the accuracy of the maxillary occlusal plane angle. The results showed obvious differences between the two methods. The casts mounted using the spirit level systems were within 1º of the patients' maxillary occlusal plane angle, whereas, the cast mounted with an orbital pointer were -10.75º and 11.5º. It was therefore evident that the spirit level facebow system, where the patients natural head position was recorded, was a more accurate system for mounting the patient's maxillary occlusal plane angle onto the semi-adjustable articulator.

Walker *et al* (2008) explained the need for an orthognathic articulator to carry out accurate surgery prediction as semi-adjustable articulators were designed for constructing dental prostheses and have arbitrary settings which do not take into account patients with

asymmetry problems. Walker *et al* (2008) designed an orthognathic articulator that worked together with an orthognathic facebow that was engineered to accommodate patients with large and significant asymmetry. The orthognathic articulators design requirements were such that the condylar components were adjustable in the vertical, anterior-posterior and lateral direction. In addition, the condylar components were also able to rotate about a vertical axis. It was also desirable to replicate the movements of the mandible by having the lower model section of the articulated cast move as opposed to the upper cast on other articulators.

In Walkers' study the orthognathic facebow was used to record the maxillary positions of twelve patients. Six had significant jaw asymmetry and six did not. The facebows were taken using a centred circular spirit level to record the natural head position. Linear spirit levels were centred on each condylar rod, to ensure the lateral condylar rods were horizontal. After removal from the patient, the facebow was adjusted by reducing the condylar connectors laterally by 10mm on each side, to compensate for the thickness of soft tissue over the condylar head. The facebow was then located on the orthognathic articulator.

The results obtained confirmed that the articulator did not show significant difference for asymmetrical and non-asymmetrical patients. When comparing the maxillary occlusal plane angle on the articulator to the posterio-anterior cephalogram there were no significance clinical differences. From this study it would appear that Walker *et al* (2008) has made considerable advancements in eliminating the errors previously associated with facebow and articulators for Orthognathic planning. However, Gold and Setchell (1983) suggested that some of the gross error in facebow transfer is due to poor understanding and insufficient practice by the individual operating the facebow. It is therefore paramount that

further studies be carried out on larger groups of patients using different operators to determine how different operators affected the accuracy of Walker's orthognathic facebow and articulator system. Other factors that could affect the results of future studies was Walker's 10mm reduction in the inter-condular rods distance to compensate for the thickness of soft tissue at the condyles head which would not be standard for all patients and could lead to error. The technique does not use skeletal registration; the planning system uses dental registrations for its prediction, which could be limiting when other skeletal factors have to be addressed.

3.5 Construction of 3D Models

Winder and Bibb (2005) stated that the construction of a 3D model requires a number of steps. A high quality volumetric 3D image of the anatomy to be modelled is required. This is processed to separate the region of interest from the surrounding tissues. Data interpolation is required to convert the image data volume into an isotropic data set for mathematical modelling. The information (data) taken by the CT scanner is converted into a different format to enable the 3D modelling computer program to produce the 3D model. It was pointed out by the authors that in order to carry out these steps the operator requires significant expertise and knowledge of medical imaging, 3D model processing, computer assisted design, manufacturing software and engineering processes. These recommendations were made also by L.C. Hieu *et al* (2005) and D.T. Pham and R.S. Gault (1997).

3.5.1 Models constructed using additive technology

Winder and Bibb (2005) explained that there are many types of rapid prototyping processes available, however the two main processes used in medicine are Stereolithography *(Figure.3.4)* and Fused Deposition modelling (F.D.M.) *(Figure.3.5).*

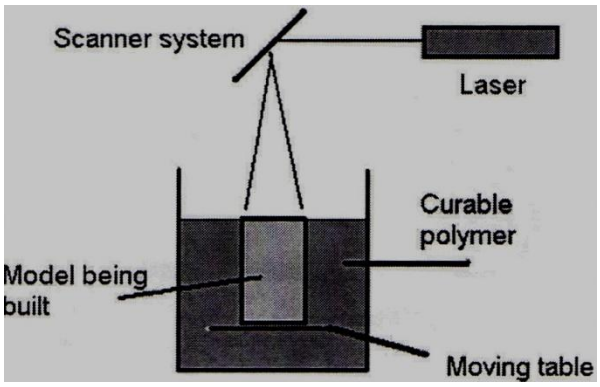

Figure.3.4 Stereolithography Modelling process.

In Stereolithography the raw data from the CT scan is in a DICOM format (Digital Image Communications in Medicine) and it is converted into an S.T.L. (Single Tessellation Language) format prior to feeding the information into the rapid prototyping machine. This slice data is then fed into the computerised rapid prototyping machine which consists of a bath of photosensitive resin, a model building platform and a ultra-violet laser for curing the resin. A mirror which is computer controlled is used to guide the laser onto the surface of the resin where it is then hardened. This process continues on a slice by slice basis until the model is complete. The layers are cured and bonded together to form a solid object, building from below to above. The resin platform is then lowered into the resin bath and a new layer of resin is wiped across the previous hardened surface using a wiper blade. This next layer is then exposed to the ultra violet laser and cured. This process is continued until the model is completed. It is then taken to the ultra-violet cabinet and cured for a further period of time.

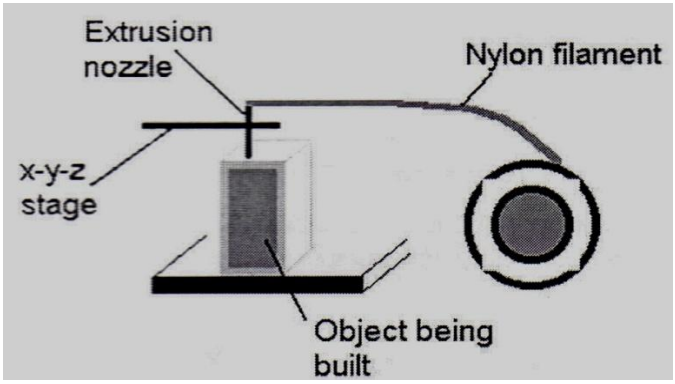

Figure.3.5 Fused Deposition Modelling process.

Fused Deposition Modelling uses a similar technique, by building the model layer by layer. The main difference is that the layers are deposited as a thermoplastic material that is extruded from a fine nozzle not unlike an electric glue gun. Acrylonitrile Butadiene Styrene (A.B.S.) is the most widely used material for building models in this fashion as it has good dimensional stability; it is rigid and relatively inexpensive. The model is constructed by extruding the heated A.B.S. from a fine nozzle onto a foam surface following a path guided by the model data. When a layer has been deposited, the nozzle is raised on top of the previous layer, where the next layer will be deposited. This is repeated until the model is completed. Support structures are needed for the constructed models and are added at the design stage; they are made of a different thermoplastic material to the model and are applied from a second nozzle; this is to allow support for the over-hanging areas of the model. These structures are then removed once complete curing of the model has taken place. There are however support structures that are made of a soluble material which would dissolve when immersed in a water bath. This process would obviously save on construction time and reduce the risk of any possible damage that might be encountered when removing these structures by hand. Winder and Bibb (2005) indicated other features that would speed up model production using this form of prototyping such as multiheaded jets as opposed to a single headed jet. This enables models to be constructed more rapidly and therefore saves time and expense.

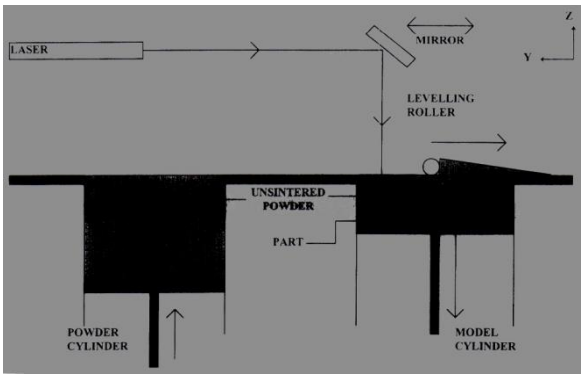

Figure.3.6 Selective Laser Sintering Modelling process.

Selective Laser Sintering *(Figure.3.6)* is a rapid prototyping technique similar to Stereolithography which uses commercially small powders of plastic, metal, ceramic or glass which are cured with an infra-red laser. The main benefit of using this method is that it does not require any support structures because the part being constructed is surrounded by unsintered powder at all times.

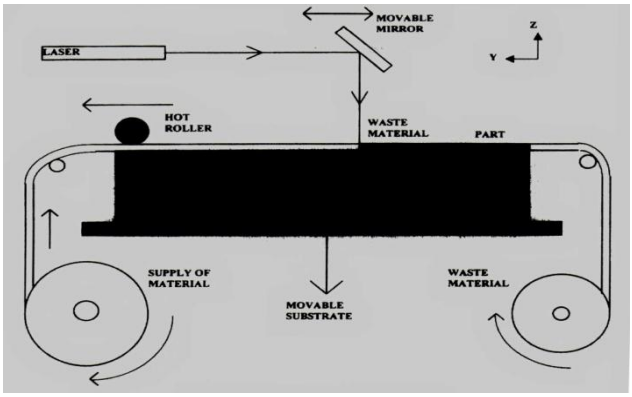

Figure.3.7 Laminate Object Manufacture modelling process.

Laminate Object Manufacture modelling *(Figure.3.7)* systems build models from layers of paper that have a heat activated adhesive on one side. Sheets are piled up one at a time as a laser cuts the outline shape. A heated roller is used to compress and activate the adhesive of each sheet bonding them together. The platform moves down once the cutting is complete to allow a fresh sheet to be rolled into place, the platform is returned to a layer below the previous position and the process starts again until the model is complete. The surplus material acts as a support for the model structure and is carefully removed once

construction is complete. This type of prototyping is very cost effective, but there are difficulties with internal voids and cavities which are often present in human structures.

3.5.2 Models constructed using subtracting technology

Another rapid prototyping system is computer controlled milling; but this technique has its limitations. Computerised controlled milling reduces a block of material to a model on a layer by layer basis, the main drawback being when a model has internal features or complex surfaces facing a number of different directions e.g. in a skull. Consequently computer controlled milling is not an ideal method for skull manufacture.

Winder and Bibb (2005) discussed problems associated with medical rapid prototyping and indicated that the imported image was the main factor for model inaccuracy. They stated that CT data did not have the same distortion as Magnetic Resonance imaging and models produced from this source had proved to be more dimensionally accurate. CT data contain a number of pixel images of slices through a human body. The pixel size and slice thickness are the key ingredients in establishing the size and scale of the data. This is calculated by dividing the field of view by the number of pixels. The field of view was determined by the radiographer at the time of scanning. Failure to have these calculated would result in an inaccurate model. A typical number of pixels in the x and y axis is 512x512 or 1024x1024.

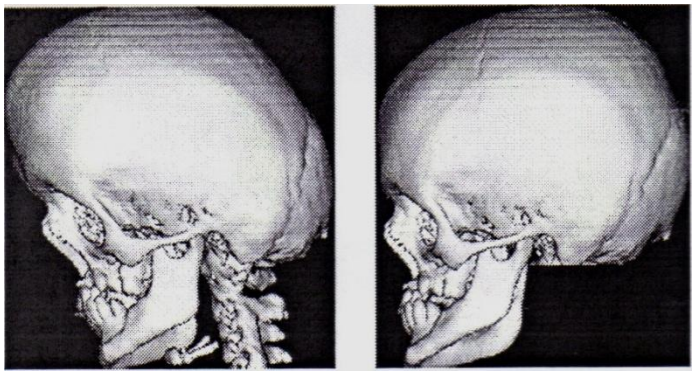

Figure.3.8 The effects of gantry tilt on the image, 15º gantry tilt on the left picture and the same skull with 0º gantry tilt right.

Numerical error in these parameters will produce inaccuracies when the data is being translated from one format to another, resulting in a wrongly scaled model. Errors in slice thickness would lead to incorrect scaling of the third dimensions again leading to distortion of the model. It is also important to have the correct gantry position prior to CT scanning *(Figure.3.8)*; failure to do so results in distortion of the image data and leads to misalignment of the slices again producing an inaccurate model. Other problems are the various artefacts that could cause difficulty when producing a 3D model. Metal artefacts are usually found in the maxilla and mandible areas due to dental fillings and other metal restorations as well as plates and screws. *(Figure.3.9)*

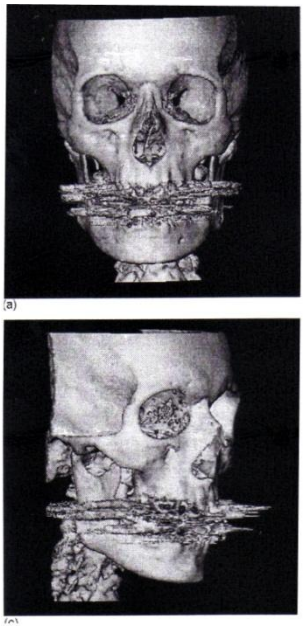

Figure.3.9 Artefacts due to dental restoration and orthodontic brackets.

These artefacts produced scatter rays around the maxilla and mandible. The scatter rays can be removed slice by slice with editing of the original CT scan image. Movement artefact occurs when a patient is restless at the time of image acquisition. The size of movement during the scan shows up as movement artefact on the model giving an obvious error in model dimensions. It is therefore important to have a satisfactory quality of data to ensure accuracy of the model being produced. Image threshold artefacts occur where the bone is particularly thin and when the model is constructed small holes appear. Bone has a CT number range from approximately 200 to 2000 Hounsfield units; this range was unique to bone within the human body. When thresholding the CT data with conversion software, a new CT number value is determined and if different from the original range, this can cause thin bony areas to be lost when the 3D model is produced. The authors conclude that image sources should be reviewed thoroughly, before image transfer and processing, because they influence greatly the quality for building and producing the model.

Choi *et al* (2002) analysed the errors in medical rapid prototyping. They used a dry human skull and made 3D virtual and rapid prototype models. Both the skull and models were

measured using several anatomical landmarks to test for the accuracy of the models. *Table 3.1 and 3.2* The landmarks were chosen as they are well understood and are widely used in clinical medicine and dentistry. They could be identified on bony surfaces and were easy to recognise and produce; this has helped to eliminate errors in the measuring process. Linear measurements were used and classified into two groups, internal measurements and external measurements. Callipers were used to record the linear distance between two landmarks on the skulls and a distance measuring function was used for the 3D virtual model using the measuring function of Magicview software programme (Materialise Belgium) to measure the same 2D linear distance points as for the skull models. *Table 3.3* The authors compared their findings to others who had carried out similar studies; Lill *et al* (1992) who produced a model from CT data by milling hardened polyurethane foam. Klein *et al* (1992) and Barker *et al* (1994) used stereolithographic models. Kragskov *et al* (1996) carried out a study on patients with four different syndromes. Since the patients' bones could not be directly measured accurately they compared the 3D visual models and the stereolithographic models. The results showed that Choi *et al* (2002) achieved better accuracy and stability in their method for producing rapid prototype models than the other quoted authors. The authors stated that using thinner layers when constructing rapid prototype models would increase the accuracy. They also reported that the CT scanning stage was of great importance as this influenced the direct accuracy of the rapid prototype model. Other factors which affected the accuracy were artefact, gantry tilt, patient movement, field of view, pixel dimensions (512 x 512). The authors mentioned the conversion from DICOM to S.T.L. file format as a possible avenue for error and they highlighted their concerns for rapid prototype manufactures. The interpolation software can have problems in its ability to deal with geometric incompleteness and surface smoothing.

Landmark	Name	Definition
Craniomaxillary complex		
ANS	Anterior nasal spine	Tip of the bony anterior nasal spine
PNS	Posterior nasal spine	The intersection of a continuation of the anterior wall of the pterygopalatine fossa and the floor of the nose, marking the dorsal limit of maxilla
ZF	Innermost point of zygomaticofrontal suture	Point at the medial margin of the zygomaticofrontal suture (bilateral)
Zy	Zygion	Point at the lateral-most border of the centre of the zygomatic arch (bilateral)
Ba	Basion	The median point of the anterior margin of the foramen magnum
Op	Opisthion	The median point of the posterior margin of the foramen magnum
FO	Foramen ovale	Point at the medial margin of the foramen ovale (bilateral)
FS	Foramen spinosum	Point at the medial margin of the foramen spinsoum (bilateral)
Mandible		
Co*	Condylion	The superior-most point on the head of the condylar head (bilateral)
Go	Gonion	The point at which the jaw angle is the most inferiorly, posteriorly and outwardly directed (bilateral)
Pog*	Pogonion	The anterior-most point of the bony chin in the median plane
Me*	Menton	The inferior-most midline point on the mandibular symphysis

*The landmarks are coordinate dependent, therefore they are marked when the FH plane of skull is positioned parallel to the horizontal plane.

Table 3.1 List of landmarks used for measurement which are co-ordinate dependant they are marked when the Frankfort horizontal plane of the skull is positioned parallel to the horizontal.

No.	Measurement	Definition	Group
Craniomaxillary complex			
1	Length of internal cranium	Anteroposterior length of the bony internal cranium	
2	Length of foramen magnum	Anteroposterior length of the foramen magnum (the distance between Ba and Op)	IMG
3	Width of foramen magnum	Longest diameter of the foramen magnum on the frontal plane	
4	ZF-ZF	Distance between left and right ZF	
5	Bizygomatic width	Distance between left and right zygion	
6	Palatal length	Distance between ANS and PNS	EMG
7	FO-FO	Distance between left and right FO	
8	FS-FS	Distance between left and right FS	
9	Bigonial width	Distance between left and right gonion	IMG
Mandible			
10	Bicondylar width	Distance between left and right condylion	
11	Ramus height (Lt.)	Distance between condylion and gonion (left)	
12	Ramus height (Rt.)	Distance between condylion and gonion (right)	
13	Body length (Lt.)	Distance between gonion and menton (left)	EMG
14	Body length (Rt.)	Distance between gonion and menton (right)	
15	Effective mandibular length (Lt.)	Distance between condylion and pogonion (left)	
16	Effective mandibular length (Rt.)	Distance between condylion and pogonion (right)	

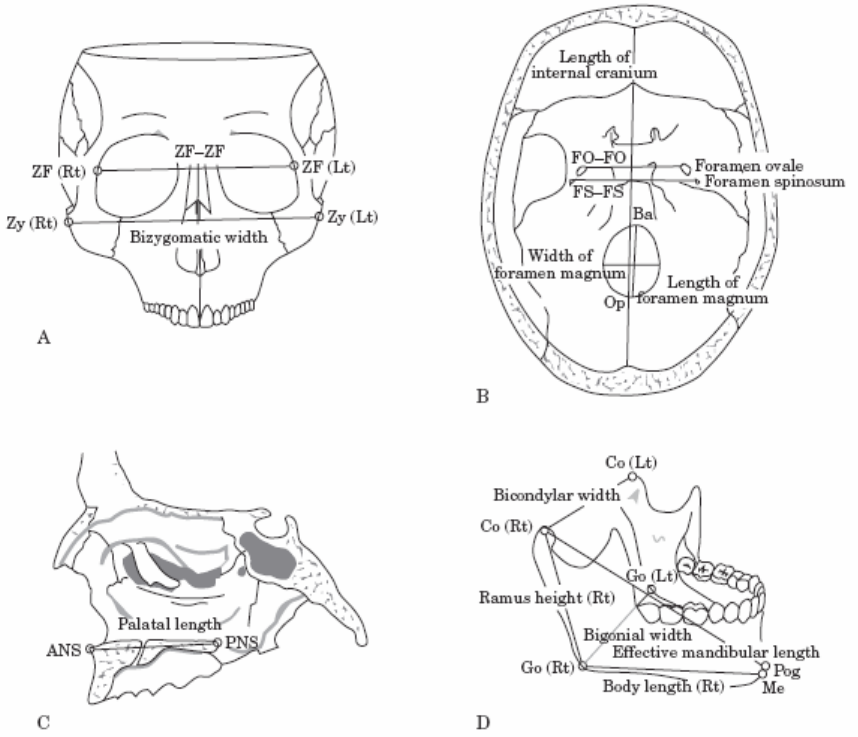

Table 3.2 Landmarks and distances measured for compairing the dimentions of the dry skull, the 3D visual model and the Rapid prototype model: Frontal view(A) Skull base (B) Sagital view (C) and mandible (D).

Table 6. Comparison with the results of other research on RP-skull differences

	Difference (mm)				% difference			
	Mean	SD	Min.	Max.	Mean	SD	Min.	Max.
Our results (Skull–RP model)	0.62	0.53	− 1.22	1.06	0.56	0.39	− 1.89	0.86
LILL et al.[8] (Skull–Milled model)	1.47	0.94	− 3.6	2.0	2.19	1.37	− 5.0	1.6
BARKER et al.[2] (Skull–RP model)[1]	1.90	1.48	− 4.62	2.8	2.54	1.38	− 3.92	3.74
KRAGSKOV et al.[6] (3-D CT model-RP model)[2]	1.98	1.20	− 1.80	5.84	3.59	2.67	− 1.85	11.33

[1]Abnormal data showing much greater % differences are removed from the calculation. The abnormality appears in thin sections, such as the lateral skull thickness.
[2]The mean and SD for all the measurement data reported in the paper. The minimum and maximum are for the averages, each of which is the mean of four syndrome cases.

Table 3.3 Comparison of other research on rapid prototype skull.

The interpolation software will estimate the increased pixel size of the raw data to fit the 3D image prior to producing a rapid prototype model which can contribute to dimensional error. Errors can also occur in the production of a rapid prototype model which included residual polymerisation, removal of support structures, laser diameter, laser path and finishing of the rapid prototype model.

Choi *et al* (2002) concluded that measurement error is inevitable including human error due to landmark location and digitisation. Incorrect calibration of measuring instruments can also affect the outcome.

3.6 Use of 3D models in medicine

Alberti (1980) was probably the first to recognise the possibility of producing 3D models from Computed Tomography scans. This process has developed and advanced over the years and it is now possible to create rapid prototype medical models from Computed Tomography Scans, Magnetic Resonance Imaging and in some cases Ultrasound. Medical Rapid Prototyping (MRP) in medicine is becoming more popular due to the reduction in cost to produce these models. They are widely used in a number of specialties, for example Orthopaedics, Neurosurgery and Maxillofacial surgery, Winder and Bibb (2005). MRP helps the surgeon to pre plan surgical procedures, these procedures can help explain the opperation to the patient, improve diagnostic ability and it acts as a guide for the surgeon during the operation helping to reduce theatre time, Terai *et al* (1999), Guyuron and Ross (1989).

There are different methods for obtaining 3D models of patients' skeletal structures. Winder and Bibb (2005) gave an account of their combined 17 years of experience

working with MRP technology. MRP is defined as the manufacture of dimensionally accurate physical models of human anatomy. These models have been used more extensively in the medical specialties of Orthopaedics and Neurosurgery. The source of image data for the creation of a 3D medical model is typically from CT scans; however, M.R.I. and Ultra sound has also been used.

The technology for producing 3D models has been available since the late 1980's, but due to production costs they have only been used in complex cases. Over time the cost of this sophisticated computer software has become more affordable and this has allowed this type of technology to be more widely available. The improvements in medical imaging technology, 3D image processing and the involvement of engineering technology methods have made it clear that this type of technology can only be of benefit to the surgeon and to the patient.

Winder and Bibb (2005) conducted a European multicentre study. A questionnaire was sent out to members of the Phidias network, which was established in 1998. Their goal was to demonstrate the value and usefulness of individual anatomical models for complex surgical procedures. The 172 responses indicated the range of applications for 3D printed models which included, the following: to aid the insertion production of surgical implants, to improve surgical planning, to act as orienteering aids during surgery, to act as a diagnostic aid, to provide preoperative simulation, to show patients what can be achieved prior to surgery as well as to prepare templates prior to resection. They also included the use of 3D models for the diagnosis of the extent of tumours (19.2%), congenital deformity (20%), post-traumatic deformity (15%), dento-facial problems (28.9%) and others (16%).

Petzold *et al* (1999) used over 200 medical rapid prototype models for aiding the correction of facial Craniosynostosis, Aperts syndrome, Otomandibular dysostosis, Hemifacial microsomia and Traumatology. The authors claimed that surgeons would be able to practise on the model with their usual surgical tools which allowed for the rehearsal of different surgical approaches. As a result of this tactile opportunity with the model it was suggested that this out-weighs the visualised model on the screen monitor, due to its ability to "touch and comprehend" allowing the surgeon to carry out a realistic simulation. Petzold *et al* (1999) claimed "The 3D model was often superior to a mere 3D visualisation because it enabled the surgeon to answer important questions during surgical simulation that defined the intervention strategy and minimised the need for ad-hoc decisions to circumvent unexpected intra operative problems."

3.7 Use of 3D models in Orthognathic Surgery

MRP, is relatively new in the field of orthognathic surgery planning; 3D printed skull models were described as far back as 1989 by Guyuron and Ross. They described their experience of using pre-surgical skull models for the planning of accurate cranio-maxillofacial surgery on 22 patients. The authors believed that due to the expense of producing these models they should be used primarily in cases with complex asymmetric, maxillofacial and craniofacial disharmonies. Guyuron and Ross (1989) explained the advantages of using 3D printed models, to outline the anatomy of the surgical site and how this could help to avoid unexpected problems. It could reduce the operation time by allowing surgeons to practise and produce a plan for eliminating difficulties prior to surgery. The authors also indicated that attachments could be prefabricated, e.g. bone plates, condylar prostheses and reconstruction plates prior to surgery, thus saving time and money. In addition, the omission of the overlying soft tissue resulted in greater skeletal

exposure allowing the possibility of model surgery to be performed more accurately. However, it was noted that this would not necessarily correct soft tissue changes when there are asymmetric movements. The authors claimed that in dealing with bone tumours, 3D printed skull models were an ideal tool. A 3D printed skull model detailed the approximate extent of the tumour and could enable the surgeon to plan reconstructive measures preoperatively. The authors concluded that it would be unwise for trainee surgeons to perform a difficult surgical procedure without practicing the procedure preoperatively on the 3D printed skull models of the patient concerned. In addition, rather than practising procedures on normal cadaver skulls which did not represent the true craniofacial deformity of the patient, the surgery could now be performed and practised on the actual patients' model skulls. Guyuron and Ross (1989) stated that follow up skull models served as a comparative reference study for any growth changes that took place postoperatively, but this would require further CT scanning.

Guyuron and Ross (1989) also described the drawbacks of 3D printed skull models, for example their inability to predict how the soft tissue would respond after the correction of skeletal unbalance. Another concern was the level of radiation exposure which was greater than in routine radiograph due to acquiring information from the CT for the construction of a 3D model.

Karcher (1992) used a technique involving titanium mini-screws being inserted into the patient as points of reference to enable plaster dental casts to be inserted into a 3D model. The screws were inserted under local anaesthetic and then a CT scan was taken using 1.5mm slice thickness with the titanium screws in position. The Zygomatic-alveolar crest and the nasal aperture were the preferred sites for screw attachment. The titanium mini-screws had no artefact in the 3D visualisation of the patients CT data, therefore they were

ideal as a marker for this purpose. The CT data was converted to produce a life size model of the patients' skull from a milling technique known as a "Styrodur" model. The milled model was attached to a platform prior to removal of the 3D milled models dentition. A splint was constructed with the upper and lower indentations marks with 3 strong metal wires, the ends of which were positioned in the middle of the cross on the screw. The plaster dental models were placed into the prepared splint and located using a device that is fixed to the three reference points (titanium mini screws) with two further arms fixed to the supraorbital rims of the patient.*(Figure.3.10),(Figure 3.11) and (Figure. 3.12).*

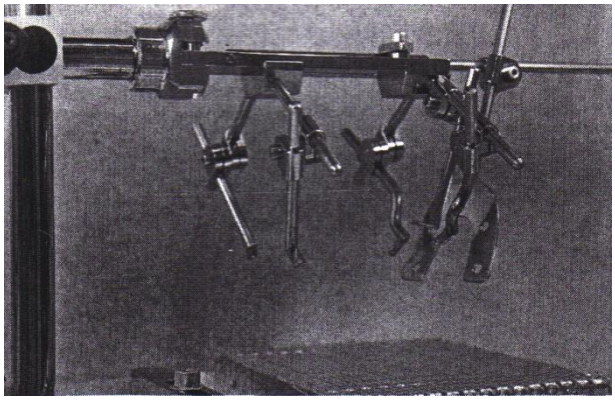

Figure.3.10 The transfer device, with two arms for supraorbital fixation and three arms for fixing to the reference screws.

Figure.3.11 The transfer device detached from the main platform ready for use.

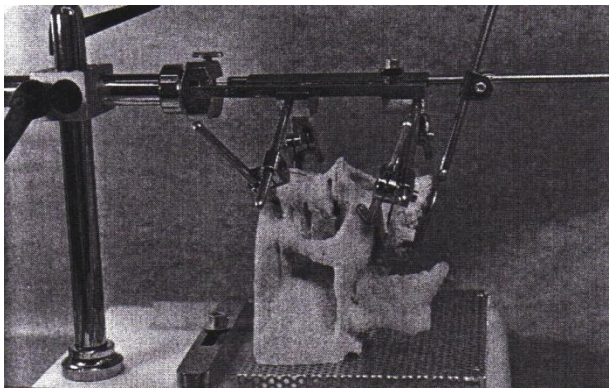

Figure.3.12 New maxillary position attached to the transfer device.

With the reference arms clamped in their positions, the device was removed from the patient and transferred to the milled model attached to the platform for positioning of the plaster dental arches. The wires on the occlusal splint are located on the mini-screws on the milled model. Once the position was achieved the device was removed. The milled model was then used to predict the new maxillary position. The device was sterilised and used to reposition the patients' maxilla in theatre. The teeth of the maxilla were positioned onto the bite arm. The arms of the device were secured to the reference points (titanium mini screws and supraorbital rims) the maxilla was placed into its new position and held with mini plates and screws. The device was removed and the mandible was osteotomised and fixed to the maxilla to the desired occlusion. The author declared that the mini screws on the milled model were within 1mm of accuracy to those on the patient. He stated that the patients' anatomy was successfully transferred to the milled model as the technique was confirmed during surgery. Karcher (1992) highlighted that more complicated movements involve more precise planning, as opposed to conventional methods. Simple movements can be planned using cephalometric analysis and plaster models. The author claimed that a 3D visualisation or an individual 3D model of the patient, where the dentition is involved, is useless unless the correct proportional dentition is integrated. The author stated that the transfer device was highly accurate; but there was no real evidence of the level or measure of this accuracy other than the titanium mini screws being out of alignment by 1mm. The

author admitted the operation is prolonged due to the use of the transfer device. This is unfortunate as 3D models should shorten theatre time due to the preplanning that can be carried out prior to surgery.

Fuhrman *et al* (1994) developed a technique to attach dental casts onto a 3D-CT milled model of a patient with an asymmetric deformity. The skull model was milled using a milling technique as described by Lambrecht and Brix (1990). The dental casts were replaced on the milled model. Reference points were marked anatomically using a template *(Figure.3.13)* to ensure the vertical, sagital and transverse dimensions of the casts in the model skull were correct.

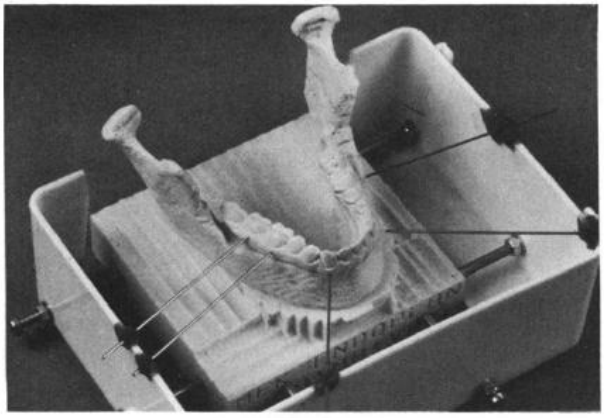

Figure.3.13 Specialised transfer template.

The mandibular section of the skull model had wires of fixed length passing through the condyle and coronoid process to attach it to the base of the skull. *(Figure.3.14).*

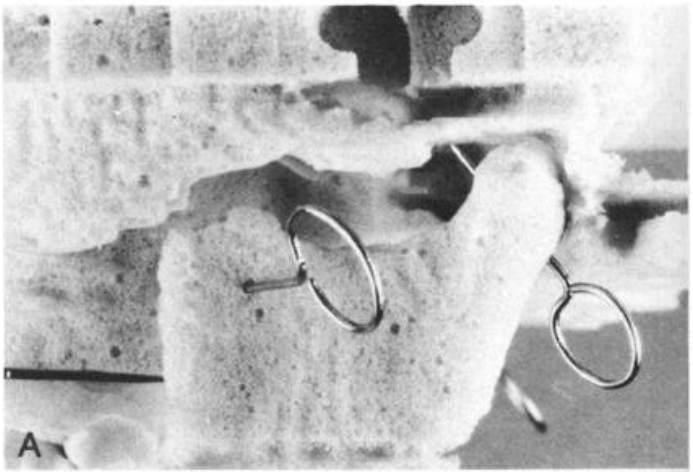

Figure.3.14 Wire attachments at condyles and coronoid process.

A second set of models were mounted on a semi-adjustable articulator after facebow transfer. To improve accuracy during the model surgery on the articulator, cephalometric distances between the maxillary and the mandibular planes to the occlusal plane were transferred to the cast models. Surgical plans were carried out on both the articulator and in the skull model. A Le Fort 1 osteotomy was carried out, with a 1mm advancement of the maxilla, impaction on the left side 3mm, downward movement on the right side by 3mm with a rotation to correct the dental alveolus to the skeletal midline. They compared the adapted milled model to the conventional surgical plan carried out on the semi-adjustable articulator.

The authors declared that the 3D model surgery with integrated models have a number of advantages as follows;

- 3D visualisation and tactile feedback.
- Assessment of the planned osteotomy.
- Assessment of the most optimal segment displacement.
- Assessment of dento-alveolar symmetry.
- Gaps at osteotomy sites with regard to bone grafting.
- Preparation of fixation devices.

Fuhrman *et al* (1994) continued by declaring that 3D models with integrated cast models of the dentition were a valuable tool for detailed treatment planning and improving the orthognathic prognosis. The present system of orthognathic planning is largely limited to only the dento-alveolar dental area. The authors conceded that the relationship of dento-alveolar structures to the skeletal base could be exactly predicted using Cephalometric distances between the maxillary and mandibular planes. They also added that a more accurate transfer of the cast models to the 3D skull model could be obtained by using a facebow transfer. The facebow would have a degree of unpredictability as a result of the variable overlying soft tissue thickness; however, it would provide a greater degree of accuracy, due to the location of anatomical points of reference. Fuhrman *et al* (1994) concluded that orthognathic planning prediction was enhanced by using 3D skull models for the correction of complex facial structures where conventional treatment planning with semi-adjustable articulators had failed to give the same quantity of information.

Studies such as Lill *et al* (1992) for milled models, Barker *et al* (1994) and Klein *et al* (1996) for stereolithographic models and Kragskov *et al* (1996) for C.T. data and 3D models showed that the difference between the 3D model and the skull is approximately 1%, which is well inside the parameters for clinical use. The authors stated that the accuracy depends on the technique for positioning the plaster casts into the 3D models. They also highlighted that others have integrated dental casts into the 3D milled models however there was no mention of the accuracy of their procedure. The authors concluded by recommending the use of facebow transfer of the casts into a 3D model together with cephalometric analysis to check for positional accuracy.

Sailer *et al* (1998) used conventional radiographs, linear CT scans, 3D CT images and twenty one rapid prototype models to pre-plan operations. The authors pointed out that rapid prototyping models only become cost efficient when they are used as a tool leading

to improvement in the quality of treatment, either by allowing more precise surgical planning, the construction of templates and for implants, or by reducing the operation time. These points were also made by L.C. Hieu *et al* (2005) who continued that for research purposes it was important to build up a collection of rapid prototype models of rare cranio-maxillofacial deformities. The authors claimed that studying the models when handling them helped to give more direct information than when simply viewed with the 3D C.T. scanned images.

Santler *et al* (1998) gave an account of 10 years experience with 541 3D skull models from 346 patients, 187 male and 159 female. Their ages varied from 1 month to 83 years. The authors stated that for diagnostic purposes each model provided additional 3D information. Prior to surgery precise measurements of distances, angles and the localisation of important structures could be mapped out exactly. Some of this information could be achieved visually from the CT scan on the screen, however, after viewing this information a decision should then be made regarding the necessity for construction of a 3D model. Other applications for 3D models were for analysis of asymmetry, simulation surgery for complex cases, reconstruction of bone defects, for providing information to patients for consent purposes, education of students in surgery simulation and also in the scientific field. Due to the reduction in cost, 3D skull models were now being used in different areas, e.g. cleft lip and palate patients where growth studies using 3D skull models were used to monitor treated cases and for orthognathic surgery, where a comparison of pre and post-operative positions would be viewed in 3D. The authors mentioned that for surgery simulations of complex cases, simulation should be performed on the 3D skull model prior to the final surgery. The authors claimed that due to the fact that the resolution of CT scanning is not set high enough to shape the teeth accurately on the 3D skull model, in all

cases where occlusion plays a role, plaster models were or should be inserted into the 3D skull model.

Santler *et al* (1998) commented on how excellent 3D skull models were for planning when the new plaster dentition had been fitted; but at no stage was information provided regarding how this procedure was carried out or how accurate the position of the plaster dental arches were on the 3D printed skull model. Santler *et al* (1998) introduced a new non-invasive method of reproducing the teeth of a 3D skull models with plaster dental casts. The procedure was tested on eight 3D milled models scanned from a plastic human skull. An inter-occlusal splint was made on plaster models and mounted in centric occlusion on the SAM articulator. Indentations of the occlusion were present on both sides of the splint. A prototype clamping fork was constructed and fixed onto three hemispheres of 18mm in diameter. The hemispheres were made of acrylic resin with plaster added to achieve radio opacity. This device was then attached to the inter-occlusal splint *(Figure.3.15)* and *(Figure.3.16).*

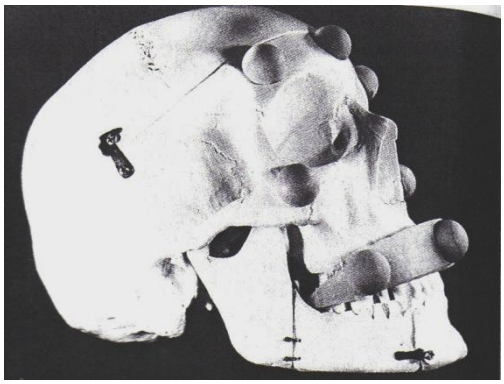

Figure.3.15 Hemisphere splint positioned in plastic skull.

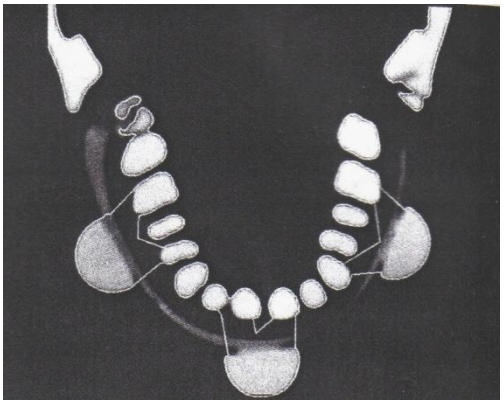

Figure.3.16 The scan with positioned hemispheres.

The authors claimed that due to the fact that the hemispheres were far enough away from the teeth, approximately 1cm, there would be no interference with artefact from any dental restorations when the technique is used in patient cases. Prior to CT scanning, five additional hemispheres were added to the malar and frontal bones on the plastic skull; these references were used to gauge the accuracy of the 3D models produced. The inter-occlusal splint was then placed into the plastic skulls dentition during the CT scanning to reduce movement artefact. The CT scanned data reproduced the hemispheres in the image as semi circles of different size. This enabled the contouring of the image to be more visible prior to model production. Five models were produced with a 3mm scan feed thickness, another three were made with 2mm, 4mm and 6mm scan feeds. The hemispheres on the 3D skull were measured prior to replacing the dental arches with plaster casts with an electronic gauge. The hemispheres appeared as a smooth surface on the 3D model and the clamping fork was fixed onto them. The clamping fork allowed reproducible opening and clamping. *(Figure.3.17)*

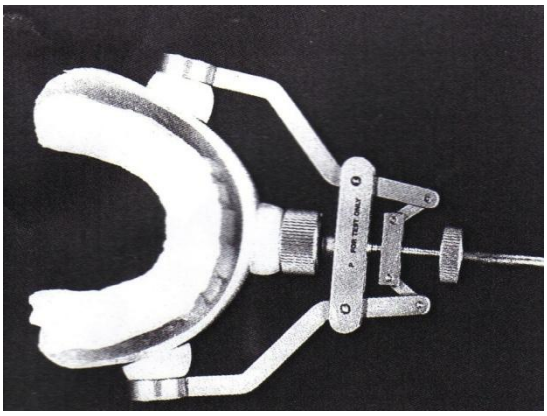

Figure.3.17 The clamping fork engaging the radio-opaque hemispheres.

The clamping fork was fixed to three hemispheres of the 3D model and to the skull to mark the position of the splint. After the clamping fork was opened, the 3D dental arch was removed and replaced with plaster models using the hemisphere splint. Electronic gauges were then used to measure the accuracy using the hemispheres as markers. The authors declared that for the 3D models made with a CT scan feed of 2mm and 3mm the hemispheres on the 3D models were easily defined and the error was less than or equal to 1mm in all directions. They stated that the mean value of 0.44mm and 0.52mm was excellent for replacing the teeth. The scan feed for 4mm and 6mm 3D models showed the hemispheres were irregular in shape indicating the higher the scan feed the more inaccurate the milled 3D model becomes in all directions. *Table 3.4* Statistical analysis of the data showed accuracy with scan distances of 2mm and 3mm (P=0.925) where as significant differences are found between 2mm and 6mm (P=0.009), 3mm and 4mm (P=0.014), 3mm and 6mm (P=0.005) and almost significant differences between 2mm and 4mm (P=0.056) In *Chart 3.1* the small box plots for 2mm and 3mm scan feeds illustrates excellent results for reproduction of the hemispheres. The larger box plots for 4mm and 6mm scan feeds illustrate that the larger the scan feed, the greater reduction in precision of the hemispheres.

	CT scan feed	2 mm feed	3 mm feed	4 mm feed	6 mm feed
Xyz	Mean deviation	0.44 mm	0.52 mm	1.04 mm	1.12 mm
	Maximum deviation	1 mm	0.91 mm	2.18 mm	2.22 mm
xy-plane	Mean deviation	0.44 mm	0.37 mm	0.48 mm	0.30 mm
	Maximum deviation	0.66 mm	0.91 mm	1.34 mm	0.73 mm
z-direction	Mean deviation	0.56 mm	0.31 mm	0.7 mm	0.69 mm
	Maximum deviation	1 mm	0.89 mm	2.18 mm	2.22 mm

Table 3.4 Measurements on models with different scan feeds.

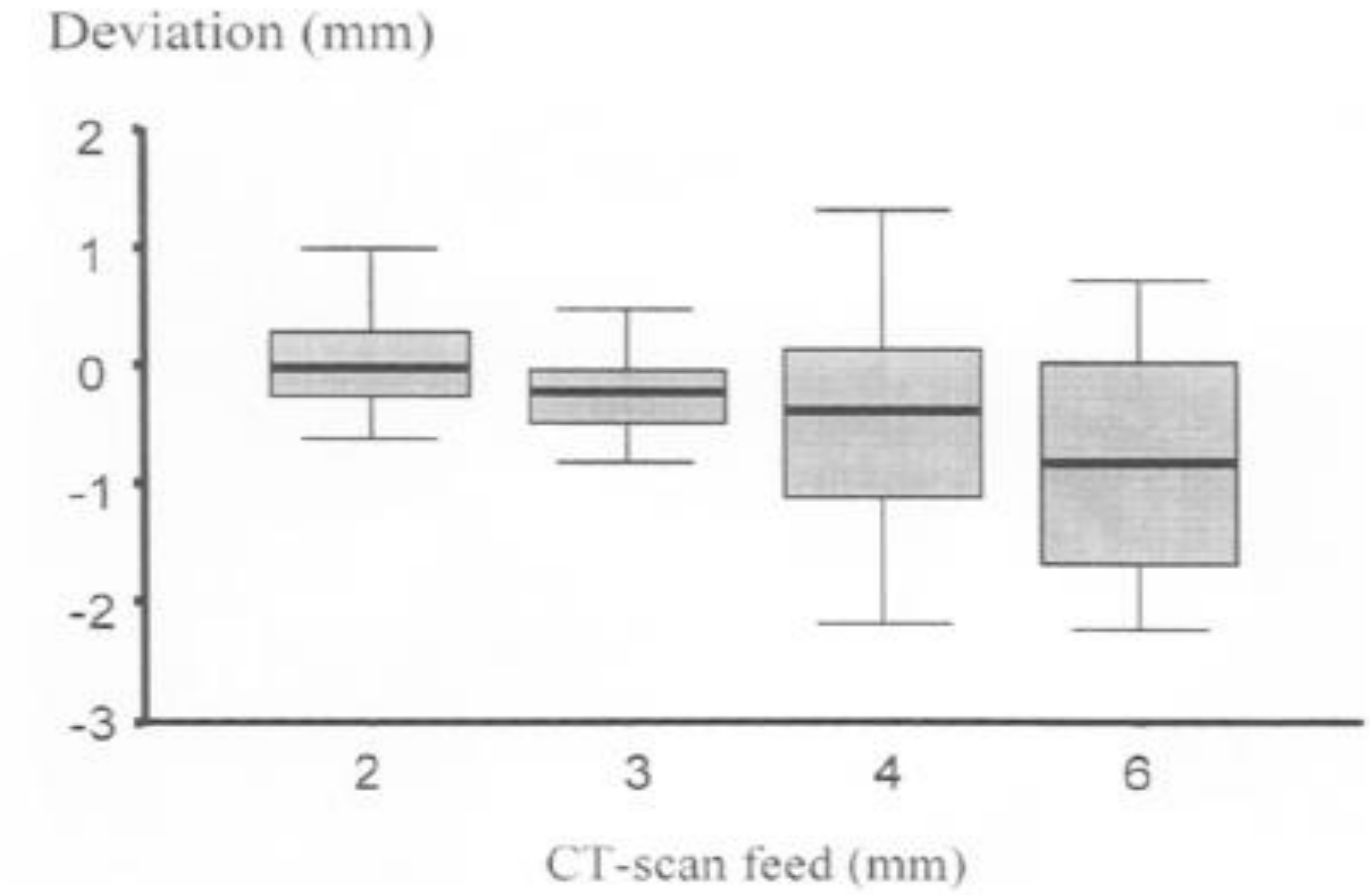

Chart 3.1 Box plot diagram showing the results with the different scan feeds.

The author concluded that the clamping fork, when positioned onto the hemispheres attached on the splint, allowed for the accurate position of the plaster cast dentition on the 3D model. However, the clamping fork will only fit when correctly positioned onto the hemispheres on the 3D model. This technique has certain problems, first, the precise accuracy of the prototype clamping fork and how it operates. Secondly, if the technique was to be carried out on patients, the positioning of hemispheres on the malar and frontal bones would not be guaranteed due to soft tissue movement of these areas. The eight models were all taken from the one plastic skull. To make this technique more robust a larger sample size and range of different skull shapes should have been scanned.

Terai *et al* (1999) investigated the errors that were present when dental casts were integrated into a 3D model skull. The authors claimed that the accuracy of the 3D models had yet to be established and stated that errors could be produced from the following;

- During CT scanning and data collection.
- During the conversion process of the CT data to allow for model production.
- Due to errors during model fabrication and the errors occurring during replacement of the 3D dental arches with plaster dental casts.

Before obtaining a CT scan, three ceramic chips measuring 3mm in diameter were pasted at 3 reference points on the face of the patient. On the upper model Nasion (N) and Nasion-Orbitale (N-Or) and in the mandible, the mandibular plane and Menton (Me). A bite fork was used to record the occlusion with a material not mentioned by the authors. The bite plate was held between the upper and lower teeth during CT scanning to maintain the same mouth opening as the bite fork produced. The CT scans were obtained with a 2mm slice thickness with an exposure time of 3 seconds. This size of slice thickness however does not follow the opinions of previous authors as they state that the thinner the slice thickness the more accurate the 3D model will be. The processing of the data was carried out on an

"Endoplan" workstation where the bone data of each slice of CT image was traced with a computer. The contour of the bone tissue including the three ceramic chips were traced on the CT image of each slice to enabled the ceramic markers to appear on the 3D model. Thin areas of bone that had shown partial volume effect or artefact from the CT image were traced manually. These slices were interpolated at 0.5mm intervals for model production using a 5 axis milling machine to make a solid 3D model. Once the 3D dentition was removed from the 3D model, the plaster dentition was integrated using a facebow transfer system. To validate the accuracy, two cephalograms were compared, one from the patient and one from the 3D model. For this to take place the model was coated with a mixture of iohexol and common paste in a 1:1 ratio to allow good exposure of the 3D model when obtaining the cephalogram. Both cephalograms were traced on the same paper with the base point and plane of each jaw being fixed. The points and planes were shown in angular and linear format and measurements were made using a protractor, callipers and a ruler measuring to the nearest ½° or 0.1mm. *(Figure.3.18)* and *(Figure.3.19).* The results of the study are shown in *Table 3.5.*

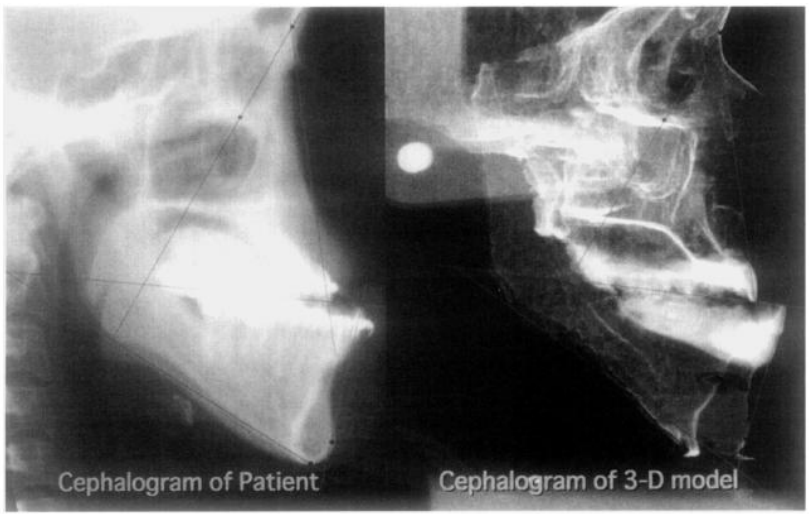

Figure.3.18 Cephalometric analysis of the patient and 3D model. Nasion (N)-Nasion Orbitale (Or) plane, Nasion (N)-Point of Upper Incisal (P.U.I. plane, occlusal plane of the upper model, Mandibular plane, Pogonion (Pog)-Point of Lower Incisal (P.L.I.) plane and the occlusal plane for the lower model.

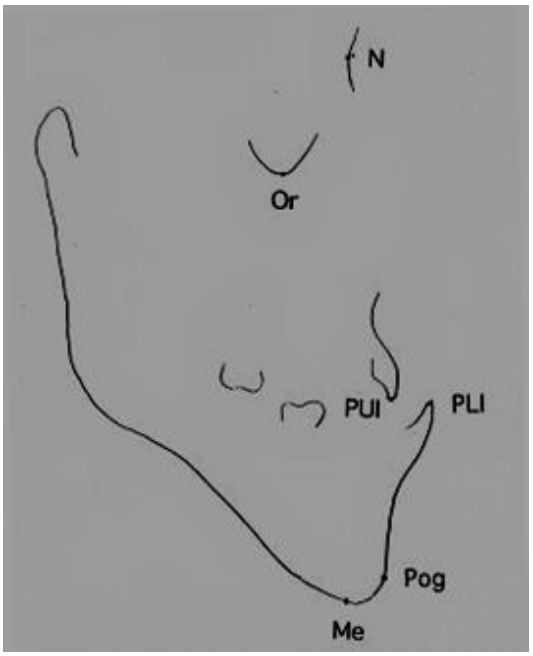

Figure.3.19 Points used in the study.

The measurement error for the (N-Or) to (N) point of upper incisor (P.U.I.) was 0.17º, (N-Or) to the occlusal plane 1º and between the point of the upper incisor (P.U.I.) was 1.23mm. In the lower the error for the mandibular plane Pogonion (Pog) to the point of lower incisor (P.L.I.) was 1º and mandibular plane to occlusal plane was 1.33º. The error between the P.L.I.'s was 1.73mm. Case number two, was a 26 year old woman with Angles class 3 mandibular prognathism and an overjet of -8.5mm with a 3.5mm overbite. The measurement error after comparison between the patient and the replicated dentition in the 3D model was (N-Or) to (N-P.U.I.) 0.83º. For (N-Or) to the occlusal plane was 1º and between the (P.U.I.) was 2.80mm. In the lower jaw the measurement error of the mandibular plane to (Pog) to (P.L.I.) was 0.00º. The mandibular plane to the occlusal plane was 2.00º and the error between the (P.L.I.) was 1.13mm. Case number three, was a 36 year old woman who had an asymmetric lower arch, with an overjet of 3mm and overbite of 3.5mm. The error between the patient and replaced 3D dentition in the 3D model was (N-Or) to (N-P.U.I.) 4.00º and for (N-Or) to the occlusal plane was 6.50º, the error between the P.U.I.'s was 6.40mm. In the lower the error between mandibular plane to

(Pog-P.L.I.) was 5.00º. For mandibular plane to occlusal plane the error was 8.67º and between the P.L.I.'s

	Case 1			Case 2			Case 3		
	P	M	Error	P	M	Error	P	M	Error
N-Or to N-PUL (°)	32.33	32.50	0.17	34.33	33.50	0.83	23.33	27.33	4.00
N-Or to Occ P (°)	76.50	75.50	1.00	72.00	71.00	1.00	85.50	79.00	6.50
PUI gap (mm)			1.23			2.80			6.40
Man p. to Pog-PLI (°)	69.00	68.00	1.00	77.00	77.00	0.00	80.33	75.33	5.00
Man p. to Occ P (°)	28.33	27.00	1.33	32.33	30.33	2.00	21.33	30.00	8.67
PLI gap (mm)			1.73			1.13			4.20

Abbreviations: P, patient cephalogram; M, model cephalogram; error, absolute value; occ p, occlusal plane; man p, manibular plane.

Table 3.5 Errors between Patient and model on Cephalometric analysis.

was 4.20mm. The results of case three showed such large errors that the cast had to be repositioned on the 3D model and re-measured. The repositioning of the cast improved the accuracy to less than 3.00º in the angular measurements and less than 2.00mm in the linear measurements. A possible cause for this could be the width of the reference points on the facial skin and movement of the soft tissue.

Terai *et al* (1999) claimed that to evaluate the accuracy of 3D models, comparisons have to be carried out between dry skulls and the 3D models of the dry skulls. Lateral cephalographs would not measure discrepancies in the medio-lateral direction which is important to evaluate.

Swennen *et al* (2007) presented on the use of a new 3D splint and double CT scan procedure to obtain an accurate virtual model of the skull with correct dental arches. The technique involves CT scanning of a patient wearing a splint which contains gutta percha markers followed by scanning the splint separately on dental casts. The two CT scans were mapped together by lining up the radio-opaque gutta percha markers on the two images virtually on the computer screen. The study was carried out on ten adult cadaver skulls with intact dentition. Impressions were taken with wax bites and plaster models were produced. Twelve gutta percha markers were placed into the splint, *(Figure.3.20)* The markers were 1.5mm approximately in diameter. Each skull was scanned with the 3D splint in position. Plaster dental casts were then scanned with the same 3D splint *(Figure.3.21)* and *(Figure.3.22).*

Figure. 3.20 3D splint with gutta percha markers.

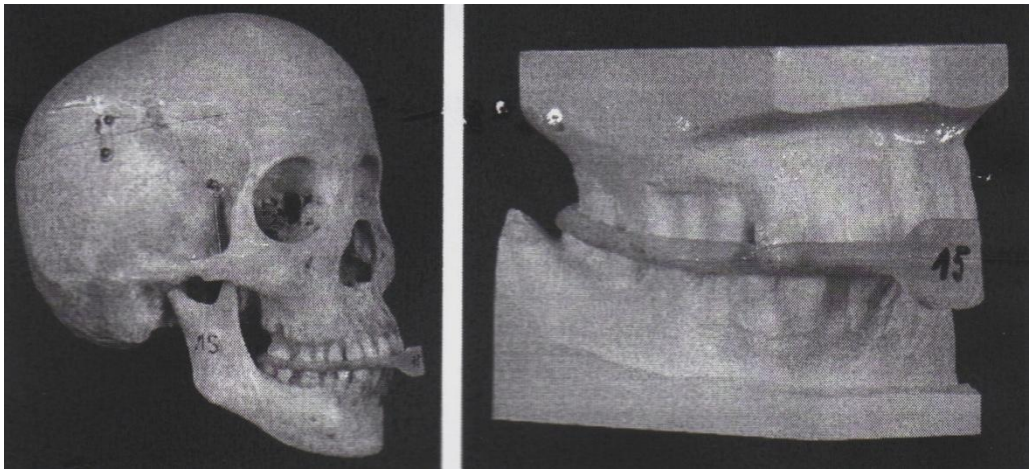

Figure.3.21 Skull with 3D splint. *Figure.3.22 Dental casts with 3D splint.*

The skulls were scanned with a slice thickness of 1mm; the dental casts were scanned at a slice thickness of 0.3mm. The CT data was then imported into viewing software. The 3D splint was used for registering and mapping the 2 CT scans using the gutta percha markers as a guide. This procedure allowed for a virtual 3D model of the skull with detailed dentition. In order to evaluate the accuracy of the process measurements were carried out for the distances between the gutta percha markers after registration.

The chosen markers used in each procedure ranged from 9 to 12mm with a mean of 9.7 ± 1.34. This was due to markers being disallowed as they touched the teeth and were engulfed by image artefact. The registration error ranged from 0.034mm to 0.3485mm. The overall mean registration error was 0.1355mm ± 0.0323mm. With a method error of registration 0.0564mm 95% confidence interval of 0.0491mm to 0.0622mm. The authors explained that the mean registration error and method error were very low and indicates many advantages of the double CT scanning technique. This included accurate integration of the dental casts into the virtual skull, detailed dental surfaces due to high resolution scanning of the plaster dental casts, reliability of 3D cephalometric landmarks, the ease and cost of producing a 3D splint for accurate segmenting of the dental arches and the ease of implementing the technique clinically. The authors highlighted some disadvantages regarding streak artefact not being totally eliminated from the soft tissue areas, the 3D splint anterior extension needs to be carefully constructed in order to avoid disrupting the formation of the lips and a good relationship with the radiological department is important for correct procedure in double CT scanning technique. The authors stated that the major drawback of virtual planning for orthognathic surgery is the inaccurate visualisation of the dental surfaces especially at inter-occlusal areas; this is due to low resolution CT scanning. The authors concluded that plaster model surgery is still necessary to establish the appropriate occlusion for surgical splints but the virtual planning of orthognathic cases will probably replace the conventional method of using dental casts. They stated that the use of Cone Beam CT scanners will become more widespread and commercially available as they have lower levels of radiation exposure and allow for vertical scanning of patients. The one drawback of carrying out orthognathic surgery planning virtually is that surgeons do not get the 3D skull model in their hand as previously described by many authors. The ability to have a tactile approach allowed the surgeon to gauge what tasks and obstacles would be expected during the operation. They concluded that this type of technique could be the

future for orthognathic surgery if more improvements in scanning and software design can be achieved.

Malivi *et al* (2007) also assessed the usefulness of bio-modelling with the intention of using them for orthognathic surgery planning. 12 patients were selected and a CT scan was taken in addition to routine preoperative cephalograms. The CT scan information was processed using MIMICS 9.22 software (Materialises' Interactive Medical Image Control System) to allow the fabrication of the 3D skull model. The skull model was produced in a Z Corporation Spectrum Z510 3D colour printer using a powder deposition modelling technique. The authors however discovered that due to the preoperative brackets on the teeth, interference occurred with the CT scan causing artefacts in both the maxillary and mandibular arches, which reduced the level of accuracy of the skull model. Added to this problem the teeth had different radiological densities to bone due to their composition and this also decreased the accuracy of the dentition. To increase the detail of the dental anatomy Malivi *et al* (2007) removed the dental arches of the 3D skull models and replaced them with orthodontic dental casts. The temporomandibular joints of the patients' 3D model were held in position in the glenoid fossa using a Kirschner wire. This ensured they maintained the correct condylar position for the patient prior to any osteotomy cuts, therefore avoiding any condylar malpositioning. For the purpose of this study, the major omission by the authors was their failure to specify their technique for replacing the dentition and to state the levels of accuracy which were obtained when the dentitions were switched. Malivi *et al* (2007) explains the orthognathic plans for their patients using 3D skull models and inter-occlusal wafers produced from articulated casts on a semi-adjustable articulator. The authors do not explain why they did not construct the inter-occlusal wafers from the newly replaced dentition on the 3D skull model. The authors concluded that operating on a 3D skull model could reflect the same scenario as in theatre

and 3D skull models are invaluable for allowing hands on experience prior to surgery. They also stated that regardless of how good 3D visual graphics are on the computer screen, a 3D skull model is an invaluable tool for surgical training as it allows surgeons to become acquainted with the anatomy of the region.

4

Technique for replacing the maxillary dentition of a 3 dimensional printed skull model (Materials and Methods)

4.1 Introduction

Three dimensional rapid prototyping is a useful means for the production of 3D models of the human skull taken from cone beam computed tomography scans. Although the accuracy of these models are acceptable, the dentition is often distorted. The aim of this study was to investigate methods to replace the inaccurately reproduced dental arches of a 3D printed skull model with accurate, correctly proportioned plaster teeth obtained from dental impressions of the natural dental arches. The intention is to use these adapted 3D printed skull models for pre-operative treatment planning and the construction of intra-operative occlusal repositioning wafers for patients with dento-facial deformities.

During the duration of this study several unsuccessful prototype methods were attempted before a satisfactory technique was determined. The various prototypes will be discussed briefly in this chapter.

4.2 Evolution of the final technique

4.2.1 Using a facebow to locate the plaster dentition onto the 3D printed skull model

The concept behind this first system was the use of a Kavo facebow (Abacus, U.K.) to record anatomical reference points on the human skull in order to make use of these as reference points to place the plaster dentition onto the 3D printed skull model *(Figure 4.1).* The reason for the Kavo facebow was the additional anatomical points which can be recorded; a typical facebow will record only three anatomical points of reference.

However, the Kavo facebow allows registration of five anatomical references points- nasion, external auditory meateae, maxillary occlusal plane, orbitale and by adding condylar extension, this also enabled registration of the condyles.

Prior to CBCT scanning, in order to assess how accurately the plaster cast dentition was replaced on the 3D printed skull model, spherical titanium ball markers (Spheric trafalgar Ashington, U.K.), 1mm in diameter, were secured to the human skull dentition. The balls were positioned on the labial and buccal surfaces of the anterior and posterior teeth. Impressions were taken of the human skulls' dentition with the balls in situ and a dental cast was produced. An acrylic occlusal wafer was constructed incorporating the incisal and occlusal surfaces of the maxillary teeth. This was placed onto the bite fork of the facebow to register the maxillary occlusal plane from the human skulls' dentition together with the other previously mentioned anatomical reference points. The human skull was then CBCT scanned and a 3D printed skull model constructed.

Figure 4.1 Kavo facebow registration of anatomical points.

The idea was to remove the dentition from the 3D printed skull models and to transfer the maxillary plaster dentition using the acrylic occlusal wafer and the anatomical references of the facebow as locators. The plaster dentition was then secured using modelling wax.

Although the technique showed it was feasible to locate the plaster dentition on the skull model, there were a number of difficulties with this technique. The main difficulty was that the facebow system could not be used if soft tissue were present, as it would be, in the case of patients. For this reason it was decided to abandon the idea and look for an alternative method for placing the plaster dentition onto the skull model. It was also interesting to note that the titanium balls had increased in size and the 3D printed skull model was larger than the corresponding human skull. The dentition of the 3D printed skull model was also seen to be visually larger

. 4.2.2 Using an intra oral splint for dentition transfer

The second method investigated replacing the inaccurate 3D printed skull model dentition using an intra oral splint and spherical titanium ball markers which were placed onto the teeth *(Figure 4.2).*

Figure 4.2 Titanium markers positioned on 3D models dentition.

After the spherical titanium ball markers were positioned on the teeth, impressions were taken of the human skull's dentition and plaster dental casts were produced. A 1mm transparent polyvinyl blank was pressure formed over the dentition of the cast models in order to create a dental splint. The 3D printed skull model was then constructed with the spherical titanium ball markers in situ. The dentition of the 3D printed skull model was

then cut away to the apical level of the titanium spheres.The polyvinyl splint was also trimmed to the apical level of the titanium sphere markers. The apical level of the titanium spheres were utilized as location points to allow the splint to be relocated; dental stone was injected into the polyvinyl pressure formed splint and allowed to set. The polyvinyl splint was then removed *(Figure 4.3).*

Figure 4.3 Injected dental stone after removal of polyvinyl splint.

This technique raised two areas of concern. Firstly, the adapted polyvinyl splint did not fit as accurately as anticipated and secondly it was difficult to inject the dental plaster into the polyvinyl splint as it did not flow into all the incisal edges and occlusal surfaces of the teeth. This resulted in large voids at the incisal and occlusal levels after the splint had been removed. Based on these previous attempts a new technique was developed in an attempt to overcome the difficulties associated with the previous methods.

4.2.3 Using gutta percha as a locating aid

The third method involved placing a gutta percha location marker onto the labial surface of the human skulls' dentition. It was hoped that the gutta percha would not magnify in the same manner as the previously used titanium balls *(Figure 4.4).*

Figure 4.4 3D maxillary process with orthodontic brackets and gutta percha.

Impressions were taken of the dental arches in the human skull with the gutta percha in position and dental casts were then produced. Pressure formed splints were then constructed encompassing the dentition and gutcha percha of the plaster model *(Figure 4.5).* The splint was carefully removed from the model.

Figure 4.5 Plaster model with pressure formed splint.

On examining the 3D printed skull model it was obvious that the gutta percha had in fact magnified during the skull production process. It appeared that anything attached to the dentition that was radio opaque would increase in size *(Figure 4.6).* Due to this magnification it was concluded that attaching gutta percha markers directly onto the tooth surfaces proved to be an unsatisfactory technique.

Figure 4.6 Magnified 3D dentition with gutta percha.

4.3 Pilot study to investigate the amount of magnification of the dentition of a 3D printed skull model

The aim of this study was to investigate the level of magnification of the dentition on the 3D printed skull model. From the previous methods detailed above it was clear that the main problem was magnification of the dental arches. Thought was then given as to how to turn this magnification to a useful advantage. In order to quantify the amount of magnification various dental and skeletal linear measurements were taken of both the human skull and its replicate 3D printed skull model *Table 4.1 to 4.3.* The human skull was scanned at 0.4mm voxel size and printed as indicated above to produce the 3D printed skull model. The measurements were taken using digital callipers (Halfords, Glasgow, U.K.) on 2 separate occasions, four weeks apart.

Measurement
Upper facial skeleton
Nasion - Anterior nasal spine
Left frontal notch - Left orbital border of zygomatic bone
Right frontal notch - Right orbital border of zygomatic bone
Widest dimensions of nasal cavity
Left frontozygomatic suture - right frontozygomatic suture
Mandible
Left tip of coronoid process - Right tip of coronoid process
Left angle of mandible - Left tip of coronoid process
Right angle of mandible - Right tip of coronoid process
Prominant point mental protuberance - Right angle of the mandible
Prominant point mental protuberance - Left angle of the mandible

Table 4.1 Measurements for the vertical dimension of the upper facial skeleton and various mandibular lengths.

Measurement
Maxilla
Left canine distal - Right canine distal
Left 1st molar distal buccal cusp - Right 1st molar distal buccal cusp
Left 3rd molar distal buccal cusp - Right 3rd molar distal buccal cusp
Mandible
Left canine distal - Right canine distal
Left 1st molar distal buccal cusp - Right 1st molar distal buccal cusp
Left 3rd molar distal buccal cusp - Right 3rd molar distal buccal cusp

Table 4.2 Measurements for the transverse dimensions at the level of the canines, first molars and third molars.

Tooth	Measurement
Right central incisor	Mesio-distal width
	Crown height
	Thickness at incisal tip
Left central incisor	Mesio-distal width
	Crown height
	Thickness at incisal tip
Right canine	Mesio-distal width
	Crown height
	Thickness at incisal tip
Left canine	Mesio-distal width
	Crown height
	Thickness at incisal tip
Right 1st premolar	Mesio-distal width
	Crown height
	Width of occlusal surface
Left 1st premolar	Mesio-distal width
	Crown height
	Width of occlusal surface
Right 1st molar	Mesio-distal width
	Crown height
	Width of occlusal surface
Left 1st molar	Mesio-distal width
	Crown height
	Width of occlusal surface

Table 4.3 Measurements for the dentition

4.4 Final method for replacing the inaccurate dentition in a 3D skull model

As a result of the previous studies the following technique was felt to be the most promising method of replacing the dental arches on a 3D printed skull model. A silicon impression of the human skulls' dentition was taken using Metrosil (Metrodent Limited, Huddersfield, England) *(Figure 4.7).*

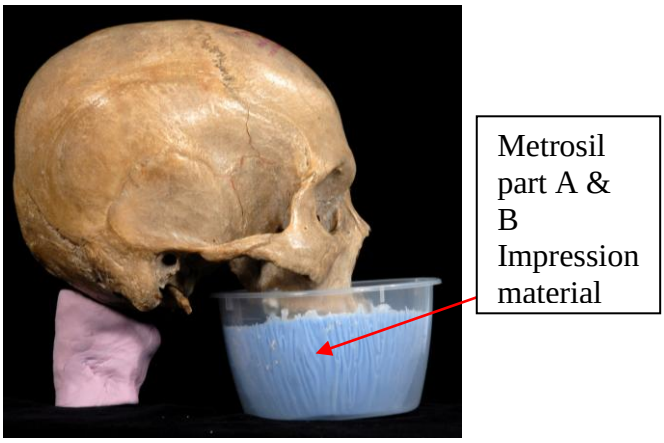

Figure 4.7 Impressions taken of dentition.

Casts of the dentition were produced using class IV dental stone (Shera Hard Rock - Shera, Werkstoff, Technologie GmbH & Co, Germany). The cast models were used to produce pressure formed splints *(Figure 4.8).*

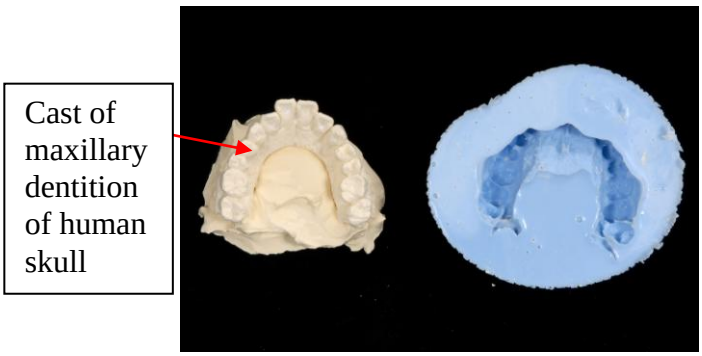

Figure 4.8 Cast model of human dentition.

A pressure forming machine, Erkodent Erkopress Es-200E (Abacus, U.K.) pressure formed a 1mm thick, 120mm diameter polyvinyl translucent disc (Abacus, U.K.) onto the dental

casts *(Figure 4.9).* The transparent disc was heated at 160º for 50 seconds at 40 pounds per square inch of pressure.

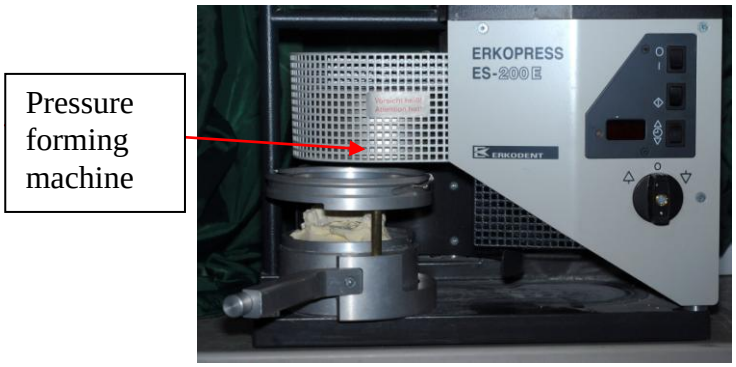

Figure 4.9 Pressure forming machine.

The polyvinyl translucent pressure formed discs were removed from the models and trimmed *(Figure 4.10).*

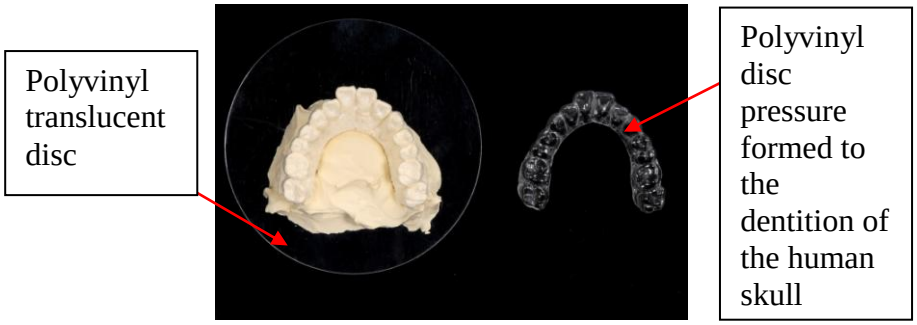

Figure 4.10 Polyvinyl splint and model.

The human skulls were scanned using the i-CAT scanner (Image Diagnostic Technology) and scanned for 20 seconds at 0.4 voxels *(Figure 4.11).*

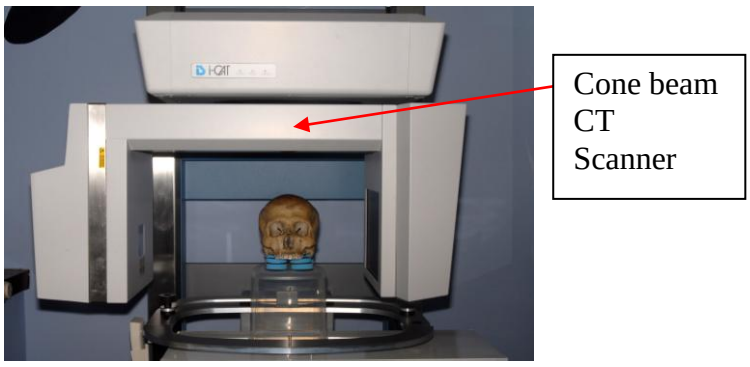

Figure 4.11 CBCT scanner.

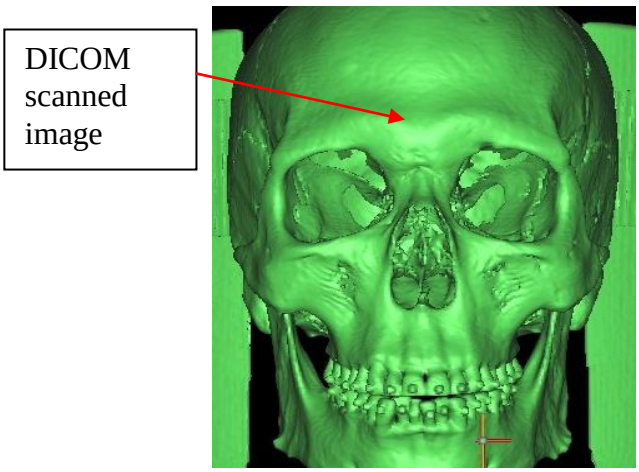

Figure 4.12 DICOM image of the skull.

This CBCT i-CAT scanned image was produced in a DICOM (digital image communication in medicine) file language *(Figure 4.12)*, this file format was then converted into an STL (Single Tessellation Language) file format for rapid prototyping using Maxilim software (Medicim, Belgium). This allowed the information to be utilised by the 3D rapid prototyping machine in order to build, layer by layer 3D copies of the human skulls *(Figure 4.13).*

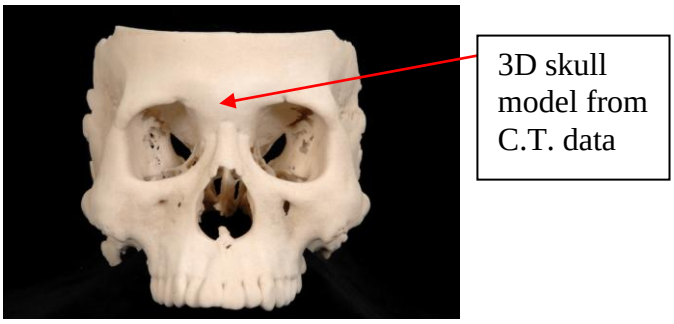

Figure 4.13 3D skull model of human skull.

The 3D skulls were made in a Z Corp 310 Plus rapid prototyping printer (Burlington, U.S.A.) using powder-binder technology which was invented and patented by the Massachusetts Institute of Technology. It took several hours for the skulls to be constructed as they were built on a 1mm thickness layer by layer basis *(Figure 4.14).*

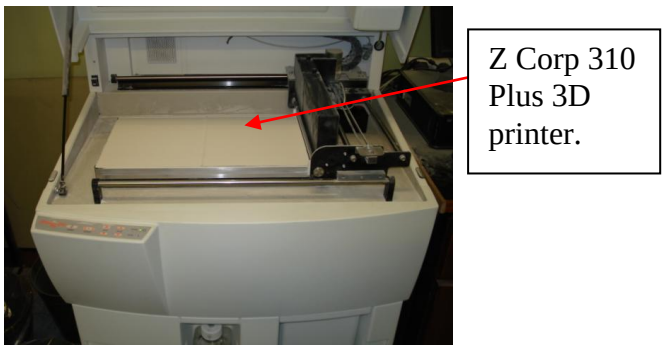

Figure 4.14 3D rapid prototype printer.

Once the 3D skull model had been printed it was attached onto a custom made platform consisting of a flat base (135mm x 127mm) and vertical column (122mm in length and 15mm x 15mm square). Two self tapping screws (Bills Tool Store, Barrowlands, Glasgow) were used to attach the base to the vertical column at 90º. A custom made halo frame was connected to the vertical column with two self tapping screws *(Figure 4.15).* This enabled the 3D skull model to be held securely using four locking pins that were attached to the halo frame.

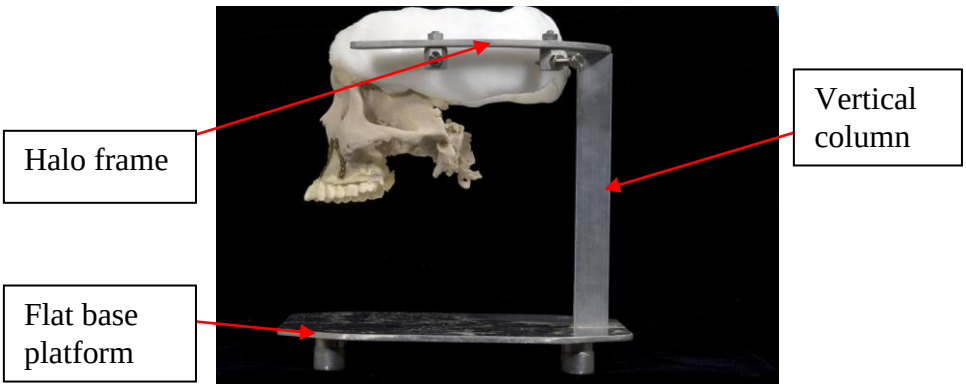

Figure 4.15 Platform for attaching skull.

Flo-Form (Bentley Chemicals Ltd, Worcestershire, England) a thermoplastic material was attached to the 3D skull model to enable it to be located and mounted onto the halo frame and to prevent damage to the skull model *(Figure 4.16).*

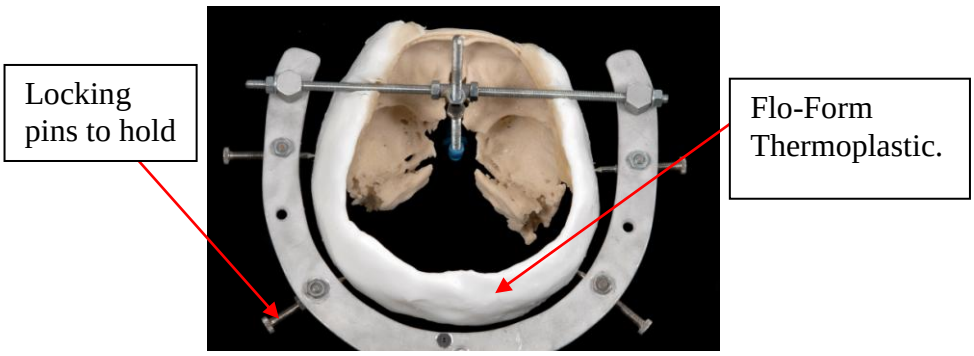

Figure 4.16 Thermoplastic material to protect skull.

Two locating plates (Synthes, Germany) were applied bilaterally onto the zygomatic buttress and to the pyriform aperture using 1.7mm screws (Synthes, Germany). Four self tapping screws were used for each plate (Figure 4.17).

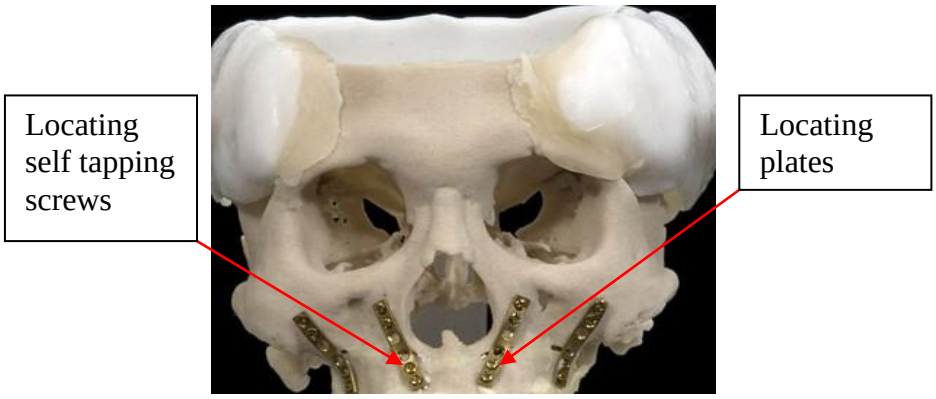

Figure 4.17 Locating plates and screws.

The 3D maxillary dento alveolar process was marked out using a pencil (W.H. Smiths, Glasgow) prior to being cut using a hack saw with a fret blade (Abacus). This permitted the 3D skull models' maxillary dento alveolar process to be removed from the base of the 3D skull model *(Figure 4.18).*

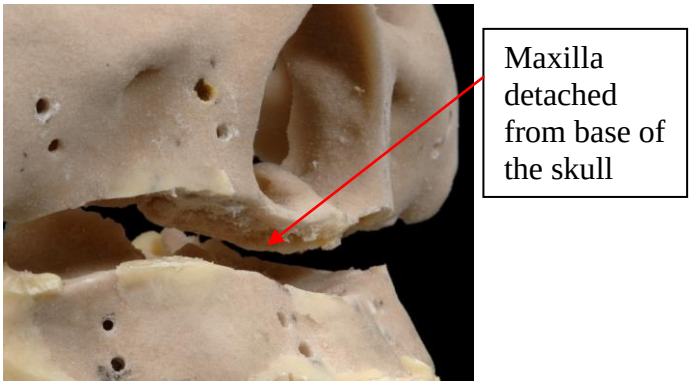

Figure 4.18 Maxillary dento alveolar process detached from the skull.

The 3D skull models' maxillary dento alveolar process were placed in the transfer jig (Dentsply, U.K.). The transfer jig had locking nuts to ensure the vertical height did not change *(Figure 4.19).*

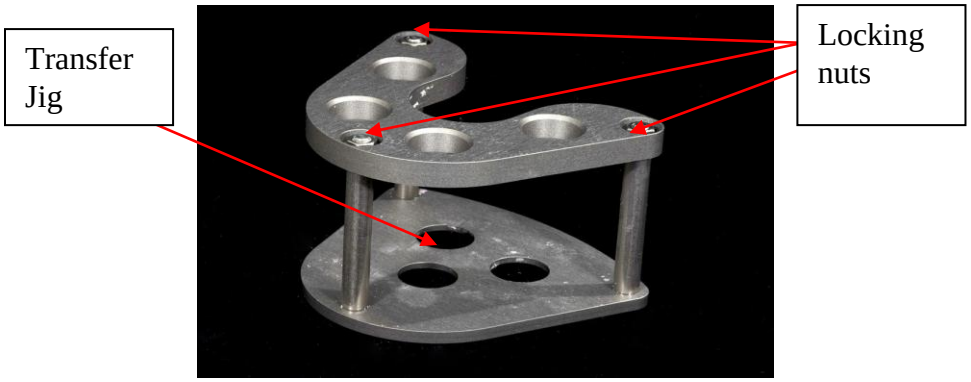

Figure 4.19 Transfer jig and locking nuts.

The 3D skull models' maxillary dento alveolar process was positioned and held in the transfer jig using a silicone compound (Coltène/Whaledent AG, Altstätten, Switzerland) *(Figure 4.20).*

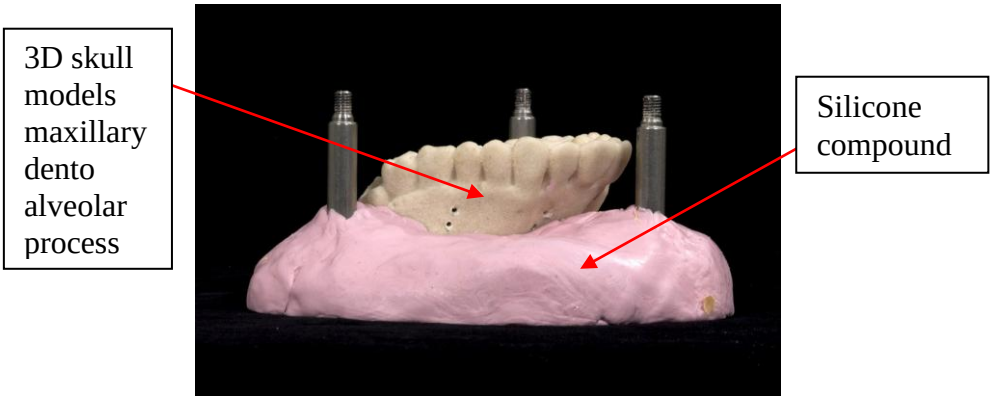

Figure 4.20 3D skull models maxillary dento alveolar process positioned in the transfer jig.

A dimensionally stable impression compound, (Alginot™ Kerr Corporation, Romulus U.S.A.) was applied to the dentition of the 3D skull models' maxillary dento alveolar process and to the top of the jig. This allowed an imprint of the 3D skull models' dentition to be recorded within the impression compound inside the transfer jig *(Figure 4.21).*

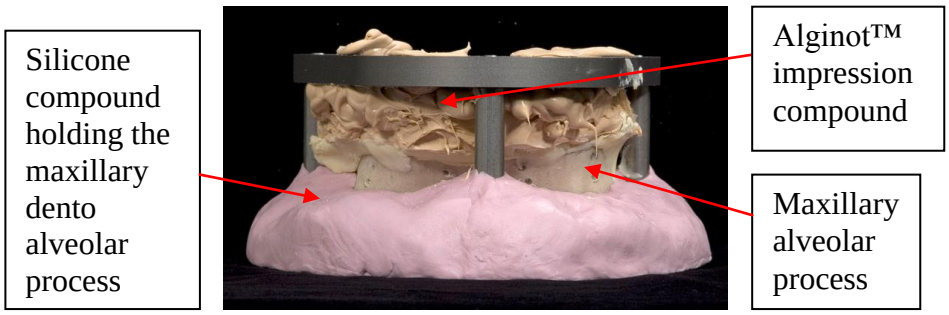

Figure 4.21 Impression material applied to 3D skull models dentition.

The previously made 1mm polyvinyl transparent pressure formed splint of the natural skulls' dentition was placed into the impression of the 3D skull models' maxillary dentition. The interior surface of the splint was in proportion to the natural skulls dentition however the exterior surface was magnified and it was this magnification which allowed the splint to fit into the impression of the 3D printed skull models' maxillary dentition. *(Figures 4.22 and 4.23).*

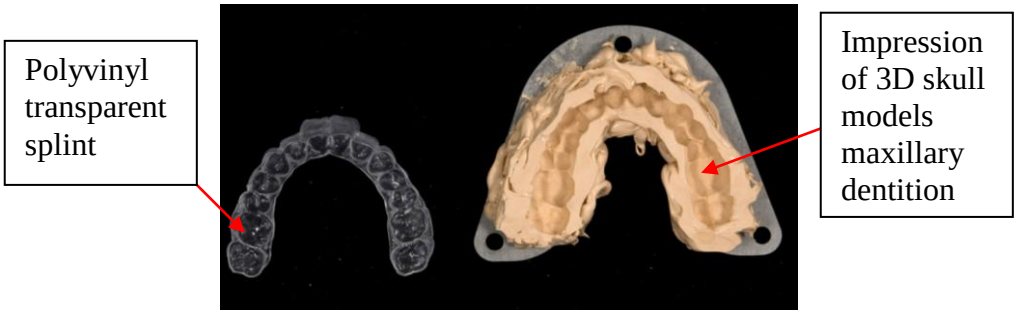

Figure 4.22 1mm polyvinyl splint.

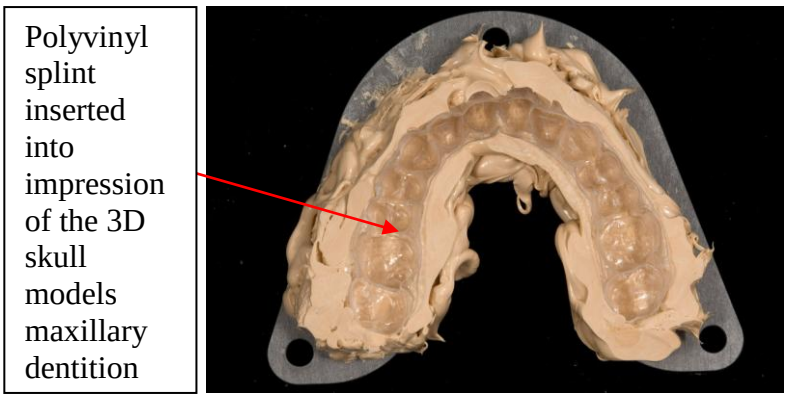

Figure 4.23 Polyvinyl splint placed into 3D skull models impression.

Class (IV) dental stone was poured into the internal fitting surface of the splint. The 3D skull models' maxillary dentition was then removed *(Figure 4.24).*

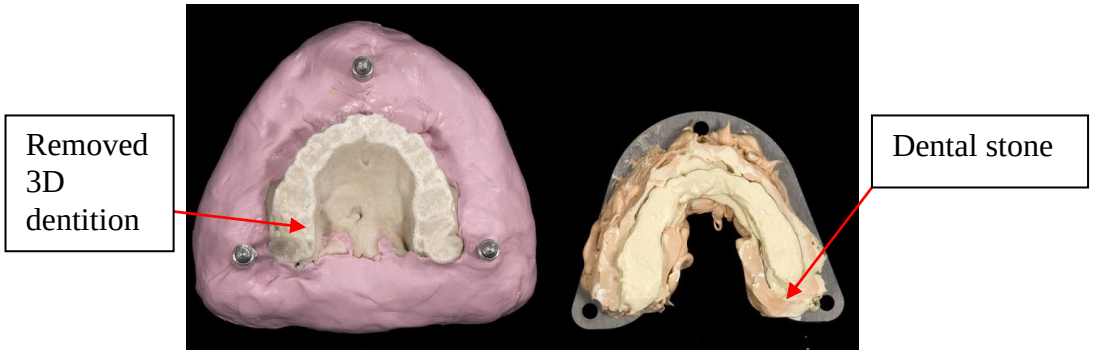

Figure 4.24 Removal of 3D skull models dentition and replacement with plaster model.

Cold cure acrylic (Metrodent, U.K) was applied to the plaster model to adhere it to the 3D skull models' maxillary alveolar process. The jig was closed and bolted to ensure the vertical dimension was maintained until the dental plaster was set *(Figure 4.25).*

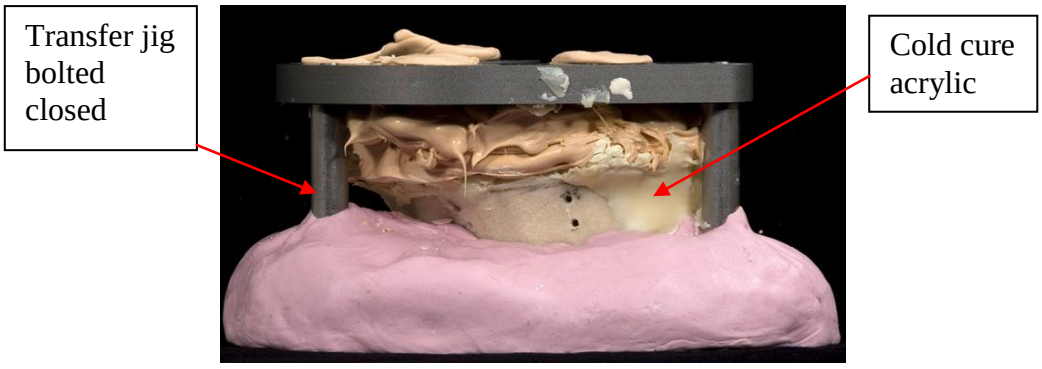

Figure 4.25 The closed jig with plaster dentition transferred.

The jig was opened and the polyvinyl splint with dental plaster dentition was attached to the 3D skull models' maxillary alveolar process *(Figures 4.26).*

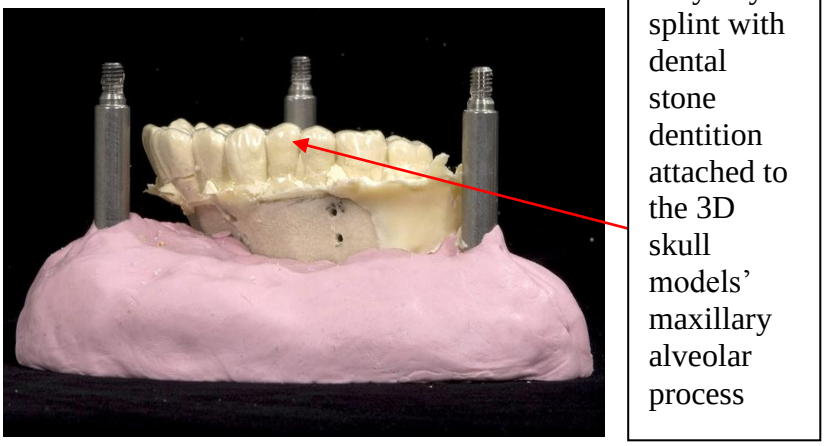

Figure 4.26 The new transferred dentition on the 3D maxillary process.

The polyvinyl splint was carefully removed from the cast dental plaster dentition. *(Figure 4.27).*

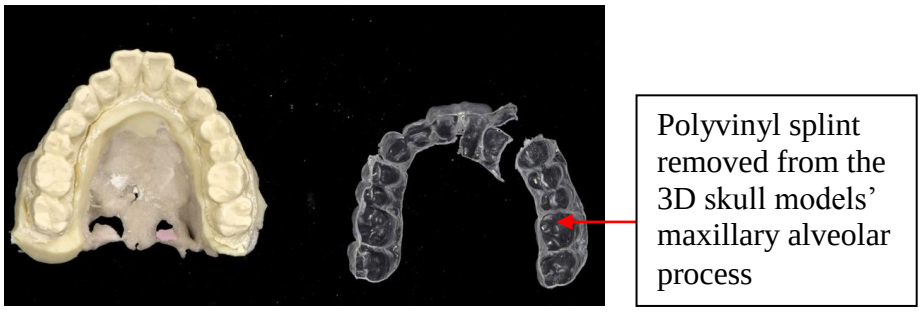

Figure 4.27 Removal of the polyvinyl splint.

The new dentition was then reattached to the skull using the locating plates and screws which had previously been adapted prior to the separation of the maxilla *(Figure 4.28).*

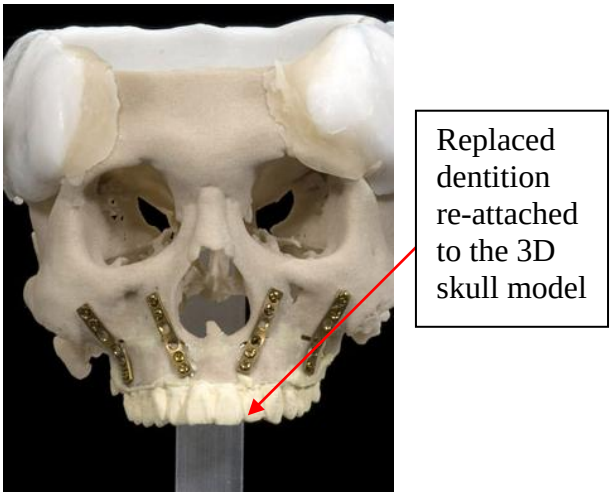

Figure 4.28 The 3D skull model with plaster dentition attached.

4.5.1 Assessment of the accuracy of replacing the dentition on 3D printed skull models

In order to determine the accuracy with which the plaster dentition was replaced onto the 3D printed skull model, both the natural skull and reconstructed 3D printed skull model were scanned using a FARO laser scanner (Scantec, Coventry, U.K.) *(Figure 4.29).* The scanner allowed 3D surface capture with an accuracy level of 0.025mm according to the manufactures specifications.

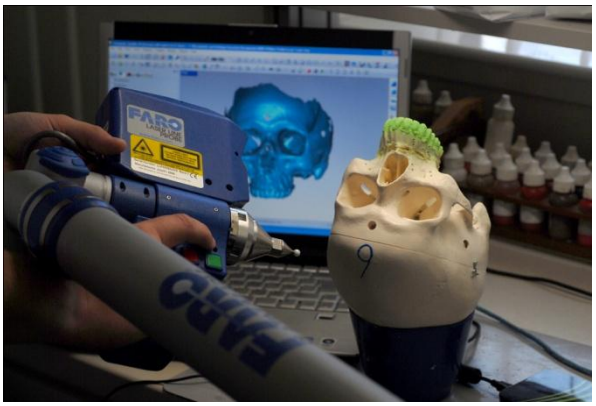

Figure 4.29 The Faro laser arm scanning a skull.

The data obtained from the scans was then imported in STL format into VRmesh software (Seattle City, U.S.A.). The computer software was capable of generating the x, y and z co-ordinates of a specific point or operator defined landmark. It also allowed the laser scanned

images of both the reconstructed 3D printed skull model and the human skull to be superimposed onto each other using specific anatomical regions.

4.5.2 Digitisation of anatomical landmarks

The landmarks on the dentition and the vault are detailed in (*Figure 4.30), (Figure 4.31)* and *Table 4.4.* For each case the 3D printed skull model and the human skull were digitised twice, one week apart; this produced 4 sets of 3D coordinates of the 13 landmarks.

1. The first set of digitised landmarks of 3D printed skull model against the first set of digitised landmarks of the human skull (Printed 1 / Human 1).
2. The first set of digitised landmarks of 3D printed skull model against the second set of digitised landmarks of the human skull (Printed 1 / Human 2).
3. The second set of digitised landmarks of 3D printed skull model against the first set of digitised landmarks of the human skull (Printed 2 / Human 1).
4. The second set of digitised landmarks of 3D printed skull model against the second set of digitised landmarks of the human skull (Printed 2 / Human 2).

Point	Landmark definition
1	Upper right first permanent molar cusp mesiobuccal cusp tip.
2	Upper right permanent canine tip.
3	Upper right central incisor mid point of incisal edge.
4	Upper left central incisor mid point of incisal edge.
5	Upper right permanent canine tip.
6	Upper left first permanent molar cusp mesiobuccal cusp tip.
7	Right Articular tubercle.
8	Left Articular Tubercle.
9	Right most inferior part of the infra orbital margin.
10	Left most inferior part of the infra orbital margin.
11	Right most lateral point of the supra orbital margin.
12	Nasion.
13	Left most lateral point of the supra orbital margin.

Table 4.4 Show the landmarks on the dentition and the vault used for superimposition and measurement.

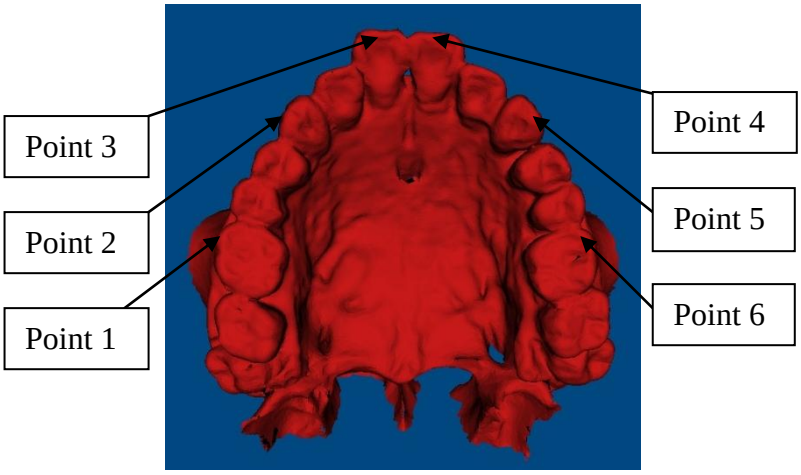

Figure 4.30 Landmarks on the natural dentition to be digitised.

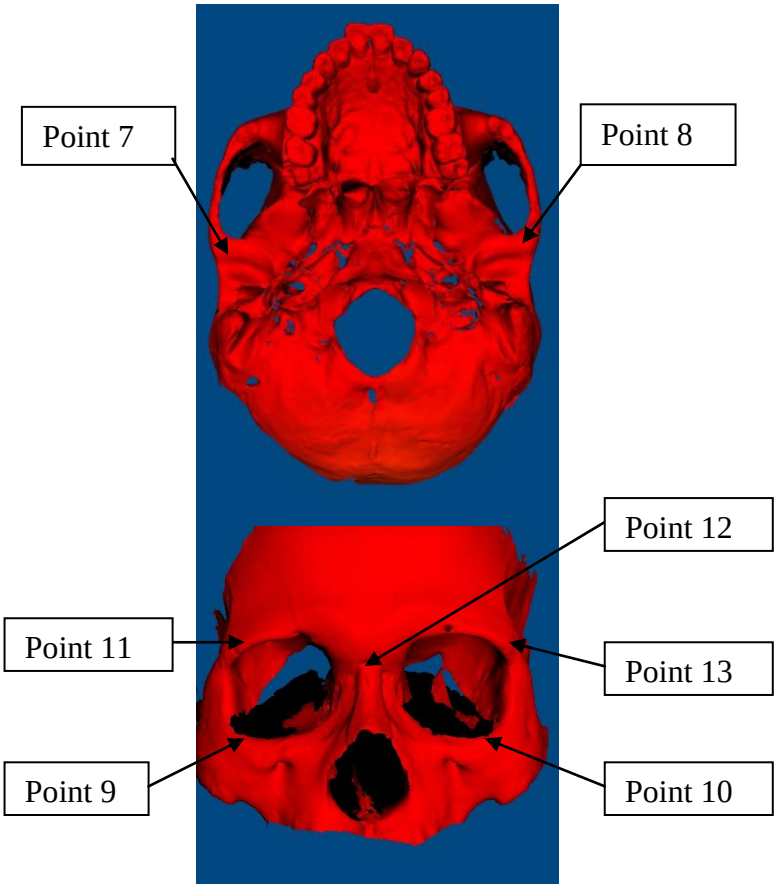

Figure 4.31 Landmarks on the human vault to be digitised.

4.6 Data analysis

In order to determine the error involved in producing and landmarking the plaster dentition, the 6 landmarks from the laser scanned human skull dentition were superimposed on the 6 landmarks of the laser scanned plaster dentition using Procrustes superimposition (Dryden and Mardia, 1998). Procrustes superimposition allowed the 3D configuration of 2 shapes to be superimposed on the geometric centre of each shape known as the centroid. This allowed each shape being superimposed to correspond to the other using the best possible alignment. The mean distance between the landmarks was calculated. The same method of superimposition was carried out for the laser scanned human skull vaults and 3D printed skull model vaults using the 7 landmarks. The mean distance between the landmarks provided information on the printing and landmarking error associated with producing the 3D printed models. The final superimposition was based on all 13 digitised landmarks. The mean distance between the 6 landmarks on the dentition was calculated as well as the mean distance between the 7 vault landmarks.

5

RESULTS

5.1 The magnitude of method error of 3D printed skull models Skeletal

Table 5.1 shows the differences in measurements between the human skull and the 3D printed skull model. The actual mean measurements of separate readings are also shown together with the standard deviation.

The differences in all the measurements were negative which indicated that the 3D printed skull model was larger than the human skull. The difference in the vertical dimension of the upper facial skeleton as measured from nasion to anterior nasal spine, left frontal notch to left orbit and right frontal notch to right orbit were 0.25mm, 0.33mm and 0.01mm respectively. The transverse differences measured at the widest point of the nasal cavity and from left frontozygomatic suture to right frontozygomatic suture were 0.37mm and 0.33mm respectively.

Table 5.1 also shows the differences between the human skull mandible and the 3D printed skull model mandible. The difference in vertical height of the ramus as indicated by left angle of mandible to left tip of coronoid process and right angle of mandible to right tip of coronoid process was 0.69mm and 1.03mm respectively. The length of the body of the mandible, left angle to left mental protuberance and right angle to right protuberance was 0.67mm and 0.40mm respectively.

5.2 Arch width

Table 5.2 shows the differences in measurements between the transverse dimensions at the level of the canines, first molars and third molars of the human skull and the 3D printed model skull. The negative values indicate that the transverse measurements of the 3D

Measurement	**Human skull**		**3D printed skull model**		
Upper facial skeleton	Mean	S.D.	Mean	S.D.	Difference between means
Nasion - Anterior nasal spine	51.6	0.2	51.8	0.2	-0.25
Left frontal notch - Left orbital border of zygomatic bone	37.0	0.1	37.3	0.2	-0.33
Right frontal notch - Right orbital border of zygomatic bone	37.5	0.1	37.5	0.2	-0.01
Widest dimensions of nasal cavity	21.9	0.0	22.3	0.0	-0.37
Left frontozygomatic suture - right frontozygomatic suture	95.3	0.2	95.6	0.3	-0.33
Mandible					
Left tip of coronoid process - Right tip of coronoid process	96.5	0.3	96.6	0.2	-0.09
Left angle of mandible - Left tip of coronoid process	64.7	0.2	65.4	0.1	-0.69
Right angle of mandible - Right tip of coronoid process	64.7	0.2	65.7	0.2	-1.03
Prominant point mental protuberance - Right angle of the mandible	85.8	0.2	86.2	0.1	-0.40
Prominant point mental protuberance - Left angle of the mandible	85.5	0.2	86.2	0.1	-0.67

Tables 5.1 Shows the differences in measurements between the human skull and the 3D printed skull model. The actual mean measurements of separate readings are also shown together with the standard deviation.

Measurement	Human skull		3D printed skull model		
Maxilla	Mean	S.D.	Mean	S.D.	Difference between means
Left canine distal - Right canine distal	37.8	0.2	38.7	0.1	-0.9
Left 1st molar distal buccal cusp - Right 1st molar distal buccal cusp	56.4	0.1	57.4	0.1	-1.0
Left 3rd molar distal buccal cusp - Right 3rd molar distal buccal cusp	65.2	0.1	65.6	0.1	-0.4
Mandible					
Left canine distal - Right canine distal	29.4	0.1	30.2	0.1	-0.8
Left 1st molar distal buccal cusp - Right 1st molar distal buccal cusp	53.4	0.1	54.1	0.1	-0.7
Left 3rd molar distal buccal cusp - Right 3rd molar distal buccal cusp	63.1	0.1	63.4	0.1	-0.2

Tables 5.2 Shows the differences in transverse measurements between the human skull and the 3D printed skull model. The actual mean measurements of separate readings are also shown together with the standard deviation.

printed skull model were larger than the human skull. The discrepancy ranged from 0.2mm to 1.0mm. There was a tendancy for a larger difference towards the front of the mouth.

5.3 Dental

Table 5.3 shows the differences in measurements between the dental dimensions of the incisors, canines, premolars and molars of the human skull and the 3D printed model skull. The negative values indicate that the dentition of the 3D printed skull model was larger than the human skull.

The upper left and right central incisors are larger mesio-distally, labio-palatally and had longer crown lengths in the 3D printed model. This difference was largest in the labio-palatal direction than any of the other dimensions. The differences ranged from 0.3mm to 1.5mm. The upper canines were larger in all three dimensions with the differences ranging from 0.4mm to 0.8mm. The first premolars were again larger in all dimensions but showed the largest differences of any of the other teeth measured, ranging from 0.6mm to 1.5mm. The first permanent molars were similar to the first premolar in size differences in the three directions measured, ranging from 0.3mm to 1.5mm.

Tooth	Measurement	Human skull		3D printed skull model		
		Mean	S.D.	Mean	S.D.	Difference between means
Right central incisor	Mesio-distal width	8.5	0.1	8.8	0.2	-0.3
	Crown height	11.2	0.1	11.6	0.2	-0.5
	Thickness at incisal tip	3.0	0.1	4.5	0.3	-1.5
Left central incisor	Mesio-distal width	8.3	0.1	9.1	0.2	-0.8
	Crown height	11.2	0.1	11.7	0.1	-0.5
	Thickness at incisal tip	2.8	0.1	4.3	0.2	-1.4
Right canine	Mesio-distal width	6.7	0.1	7.4	0.1	-0.7
	Crown height	11.8	0.1	12.6	0.3	-0.8
	Thickness at incisal tip	3.7	0.1	4.5	0.1	-0.7
Left canine	Mesio-distal width	6.9	0.1	7.5	0.1	-0.6
	Crown height	10.1	0.1	10.6	0.2	-0.5
	Thickness at incisal tip	5.1	0.1	5.5	0.2	-0.4
Right 1st premolar	Mesio-distal width	6.9	0.1	7.5	0.1	-0.6
	Crown height	9.6	0.2	10.6	0.1	-1.0
	Width of occlusal surface	8.7	0.3	9.6	0.2	-1.0
Left 1st premolar	Mesio-distal width	7.1	0.1	8.7	0.1	-1.5
	Crown height	9.0	0.1	10.4	0.2	-1.4
	Width of occlusal surface	9.2	0.1	10.2	0.1	-1.1
Right 1st molar	Mesio-distal width	9.4	0.1	10.2	0.2	-0.8
	Crown height	8.8	0.1	9.7	0.1	-0.9
	Width of occlusal surface	10.5	0.2	11.6	0.1	-1.1
Left 1st molar	Mesio-distal width	9.3	0.1	9.7	0.1	-0.3
	Crown height	8.5	0.2	9.5	0.1	-0.9
	Width of occlusal surface	10.3	0.1	11.8	0.1	-1.5

Tables 5.3 Shows the differences in measurements between the human skull dentition and the 3D printed skull model dentition. The actual mean measurements of separate readings are also shown together with the standard deviation.

5.4 Superimposition of landmarks of the human skull and 3D printed skull models

The human skull and 3D printed skull with plaster dentition landmarks were superimposed using Procrustes registration on the structures below,

- The dentition only (6 landmarks) – human skull dentition and plaster dentition.
- The vault of the skull (7 landmarks) – human skull vault and vault of 3D printed skull.
- The dentition and the vault of the skull (13 landmarks) – both entire models.

Each superimposition was carried out separately and the mean error between the landmarks recorded, *Chart 5.1* shows the results of the superimpositions. The blue circles on the horizontal line marked dentition represent the mean error between the 6 landmarks of human skull dentition and 6 landmarks on the plaster dentition following superimposition. The overall mean error was 0.55mm ± 0.37mm.

The blue circles on the horizontal line marked vault represent the mean error between the 7 landmarks of human skull vault and 7 landmarks on the 3D printed skull vault following superimposition. The overall mean error was 0.72mm ± 0.26mm.

Superimposition of the entire human skull and 3D printed skull model with plaster teeth based on the 13 landmarks was performed and the mean distances of the 7 landmarks of the vault (red circles / vault) and 6 landmarks on the dentition (red circles / dentition) were measured. This overall superimposition produced higher error measurements; the overall mean error for the dentition was 0.74mm ± 0.37mm and 0.83mm ± 0.27mm for the vaults.

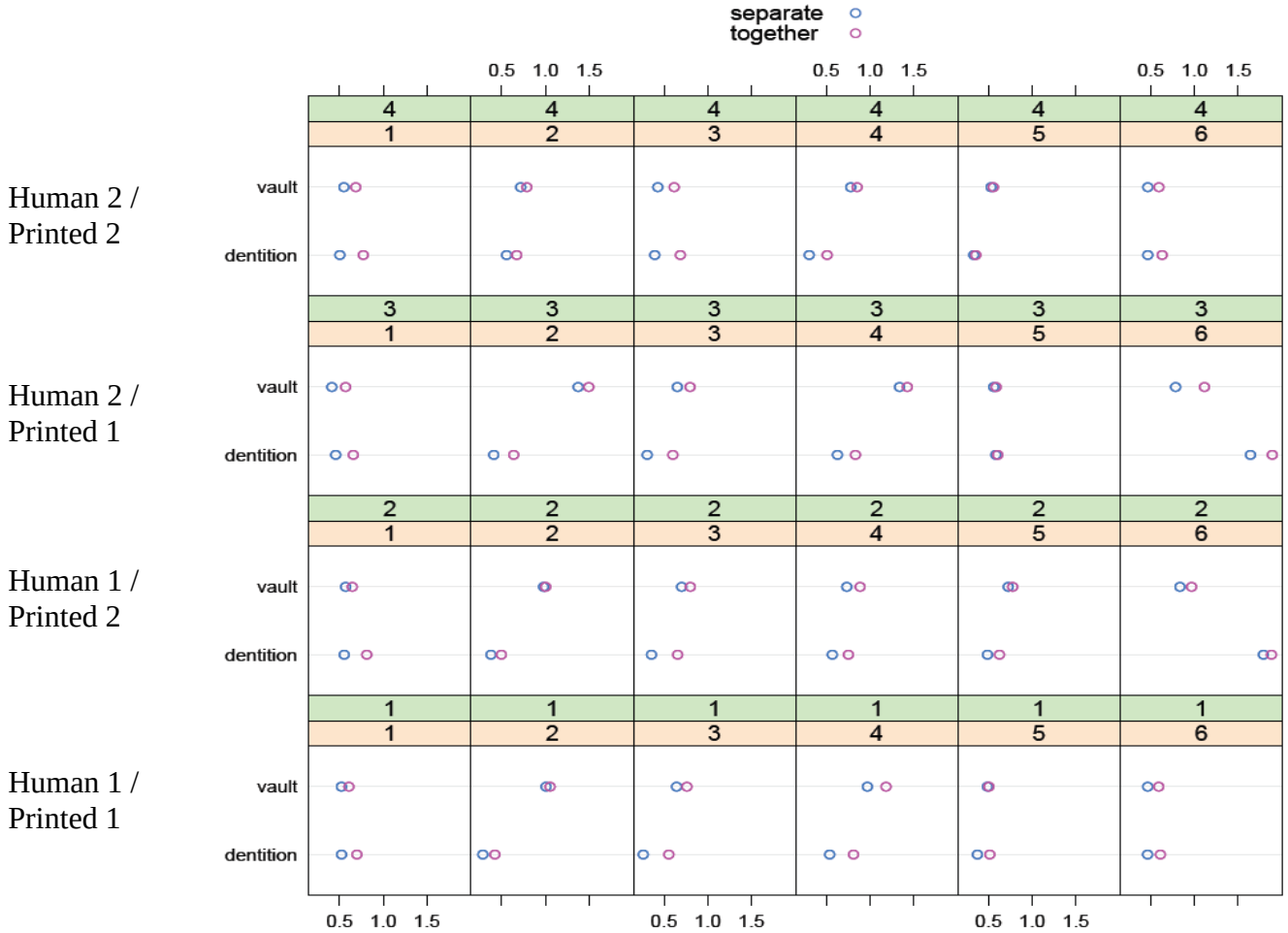

Chart 5.1 Blue circles represent the mean error between the landmarks of human skull dentition & vault and landmarks on the plaster dentition & 3D printed skull vault following superimposition. Red circles represent mean error between the landmarks of the dentition and vault when all 13 landmarks are used. Vertical columns represent the number of skulls; horizontal rows represent the superimposition sequence of the skulls.

The difference between the blue and red circles reflects the error in placing the dentition onto the 3D skull model given the fact that the vaults do not align perfectly. This is shown in *Table 5.4* for the vaults and *Table 5.5* for the dentition. The overall error of placement of plaster dentition onto the 3D printed skull model was 0.19 mm ±0.08mm. The overall error of alignment between the human skull and the 3D printed skull model was 0.11 mm ±0.07mm.

As well as superimposing the landmarks it was also possible to superimpose the laser scanned images of each of the human skull over the 3D printed model. The models were aligned using initial rigid registration followed by mesh alignment using the iterative closest point (ICP) algorithm; only the vaults were used for superimposition. *Figures 5.1 to 5.6* shows the parameters of the value indicator set between 1mm and -1mm. The green coloured parts of the images are aligned to within 0.11mm. For example skull 5 *(Figure 5.5)* shows that the frontal bones, infraorbital rims and superior parts of the zygoma are well aligned (green), but the dentitions do not align to that level of accuracy. In fact the red colour indicates the site and amount of error, with more error at the back of the dentition and a slight lateral displacement on the buccal aspect of the left dentition.

Superimposition sequence	Skull Number						Mean	S.D.
	1	2	3	4	5	6		
Human 2 / Printed 2	0.14	0.07	0.19	0.07	0.03	0.13	0.10	0.06
Human 2 / Printed 1	0.16	0.12	0.15	0.09	0.03	0.33	0.15	0.10
Human 1 / Printed 2	0.08	0.02	0.10	0.15	0.05	0.13	0.09	0.05
Human 1 / Printed 1	0.09	0.05	0.12	0.21	0.02	0.13	0.10	0.07

Table 5.4 Shows the difference (mm) between the mean vault landmark measurements when superimposed on the vaults only (7 landmarks) and on the mean full vault and dentition landmark (13 landmarks).

Superimposition sequence	Skull Number						Mean	S.D.
	1	2	3	4	5	6		
Human 2 / Printed 2	0.27	0.12	0.29	0.21	0.02	0.16	0.18	0.10
Human 2 / Printed 1	0.20	0.23	0.29	0.21	0.02	0.25	0.20	0.09
Human 1 / Printed 2	0.26	0.12	0.30	0.18	0.14	0.09	0.18	0.08
Human 1 / Printed 1	0.18	0.14	0.29	0.27	0.14	0.15	0.19	0.07

Table 5.5 Shows the difference (mm) between the mean dentition landmark measurements when superimposed on the dentition only (6 landmarks) and on the mean full vault and dentition landmark (13 landmarks).

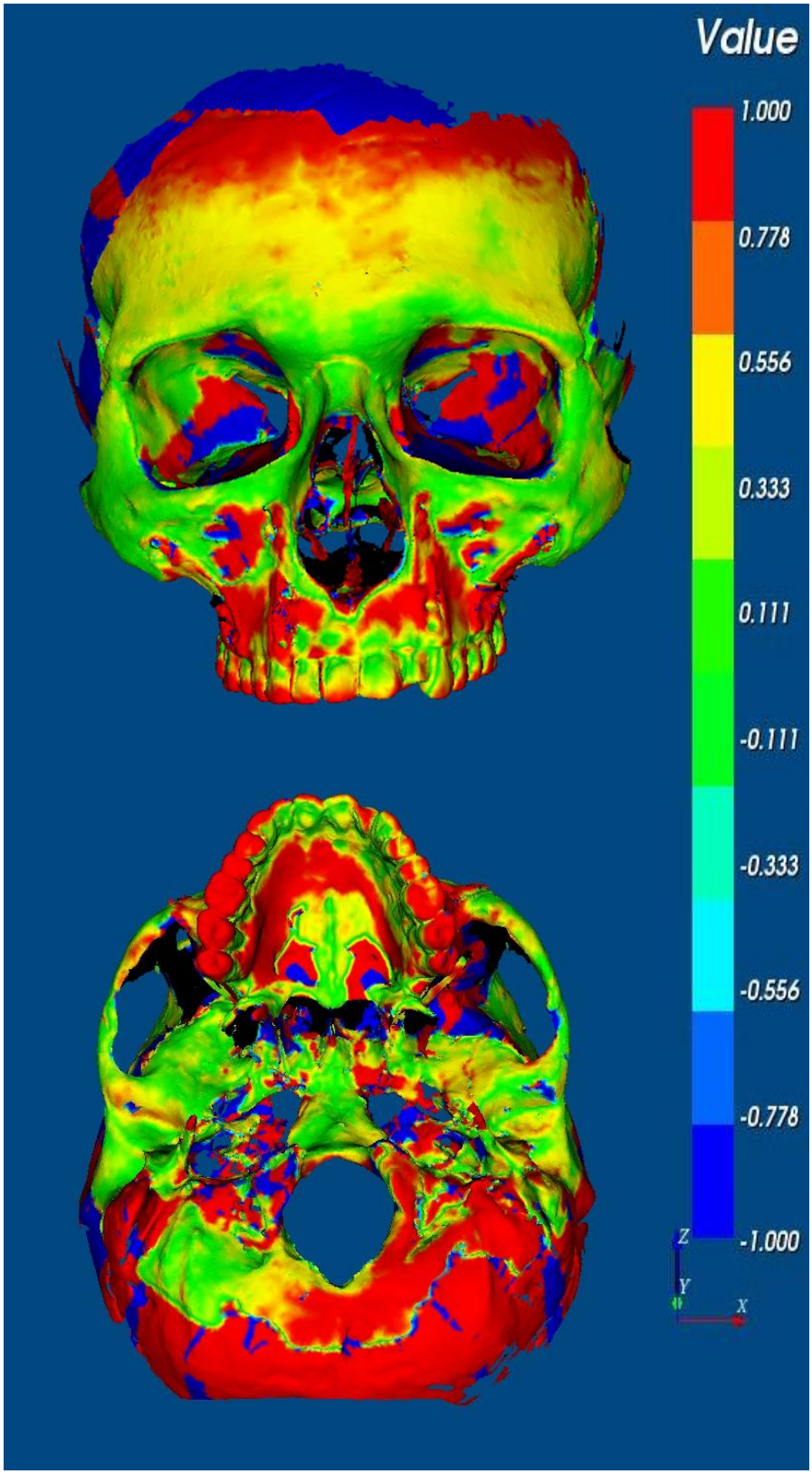

Figure 5.1 Human skull 1 mesh superimposed on the vault only of the 3D skull printed model with plaster teeth mesh using VRmesh. The distance between the meshes is indicated by the colour.

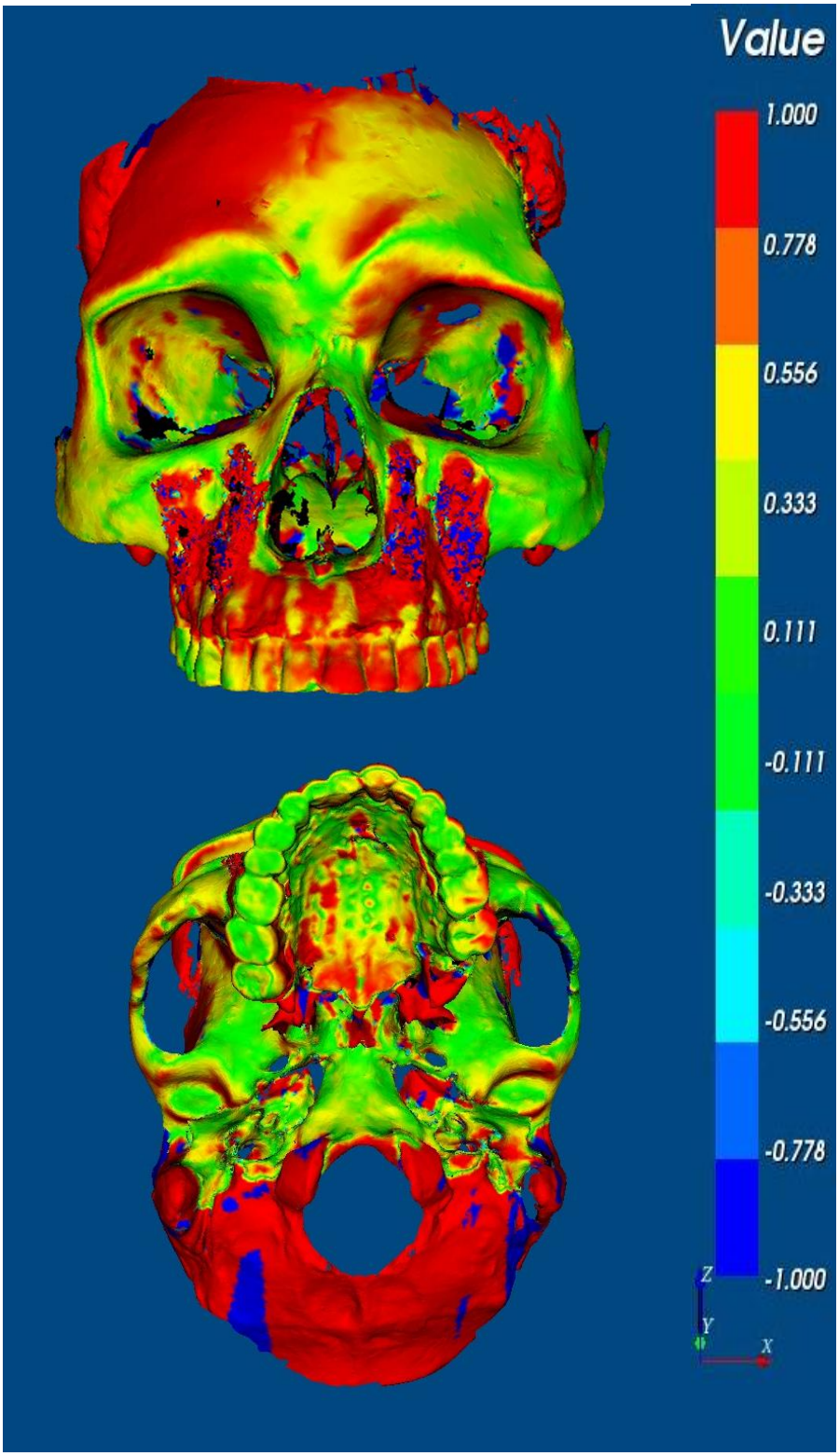

Figure 5.2 Human skull 2 mesh superimposed on the vault only of the 3D skull printed model with plaster teeth mesh using VRmesh. The distance between the meshes is indicated by the colour.

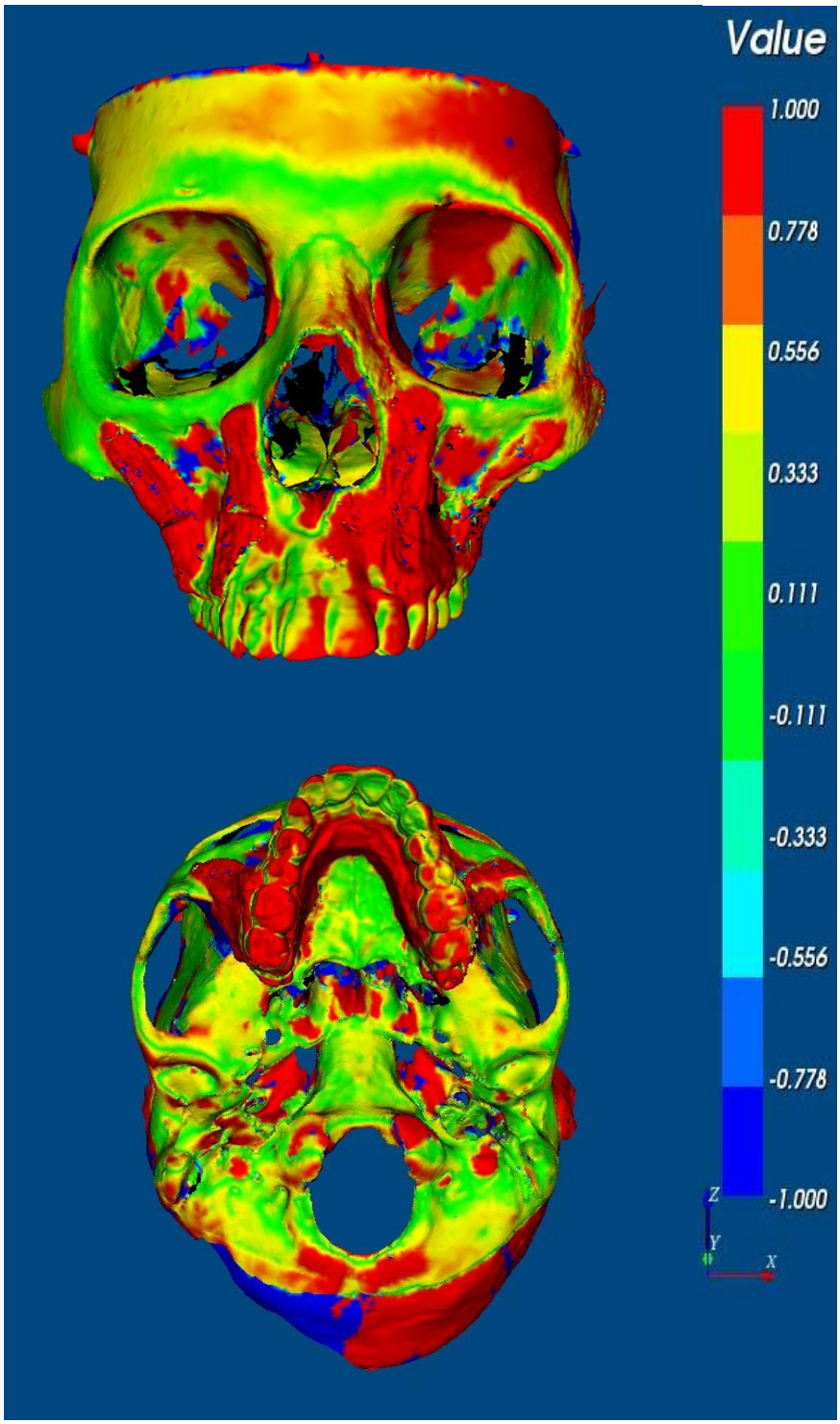

Figure 5.3 Human skull 3 mesh superimposed on the vault only of the 3D skull printed model with plaster teeth mesh using VRmesh. The distance between the meshes is indicated by the colour.

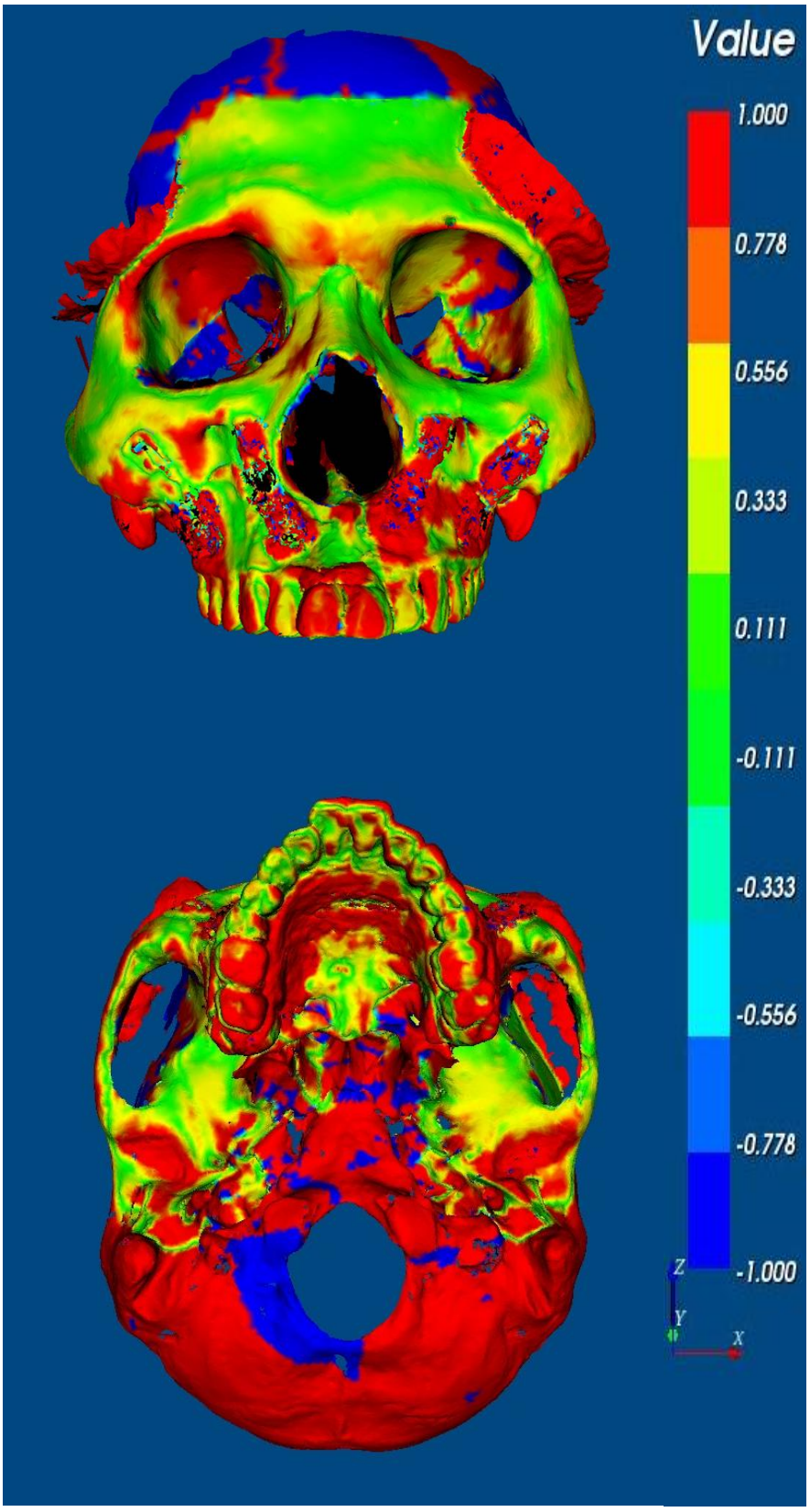

Figure 5.4 Human skull 4 mesh superimposed on the vault only of the 3D skull printed model with plaster teeth mesh using VRmesh. The distance between the meshes is indicated by the colour.

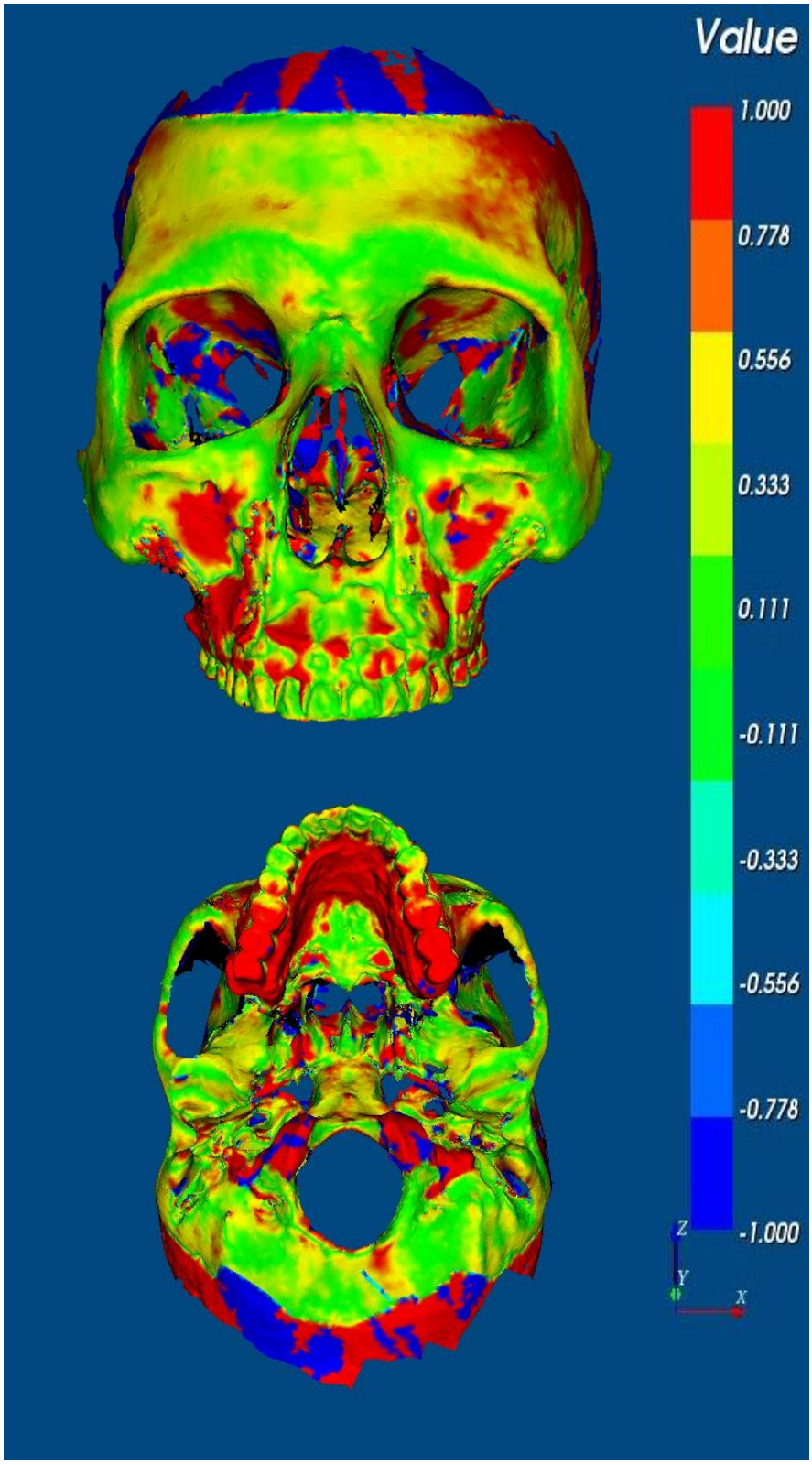

Figure 5.5 Human skull 5 mesh superimposed on the vault only of the 3D skull printed model with plaster teeth mesh using VRmesh. The distance between the meshes is indicated by the colour.

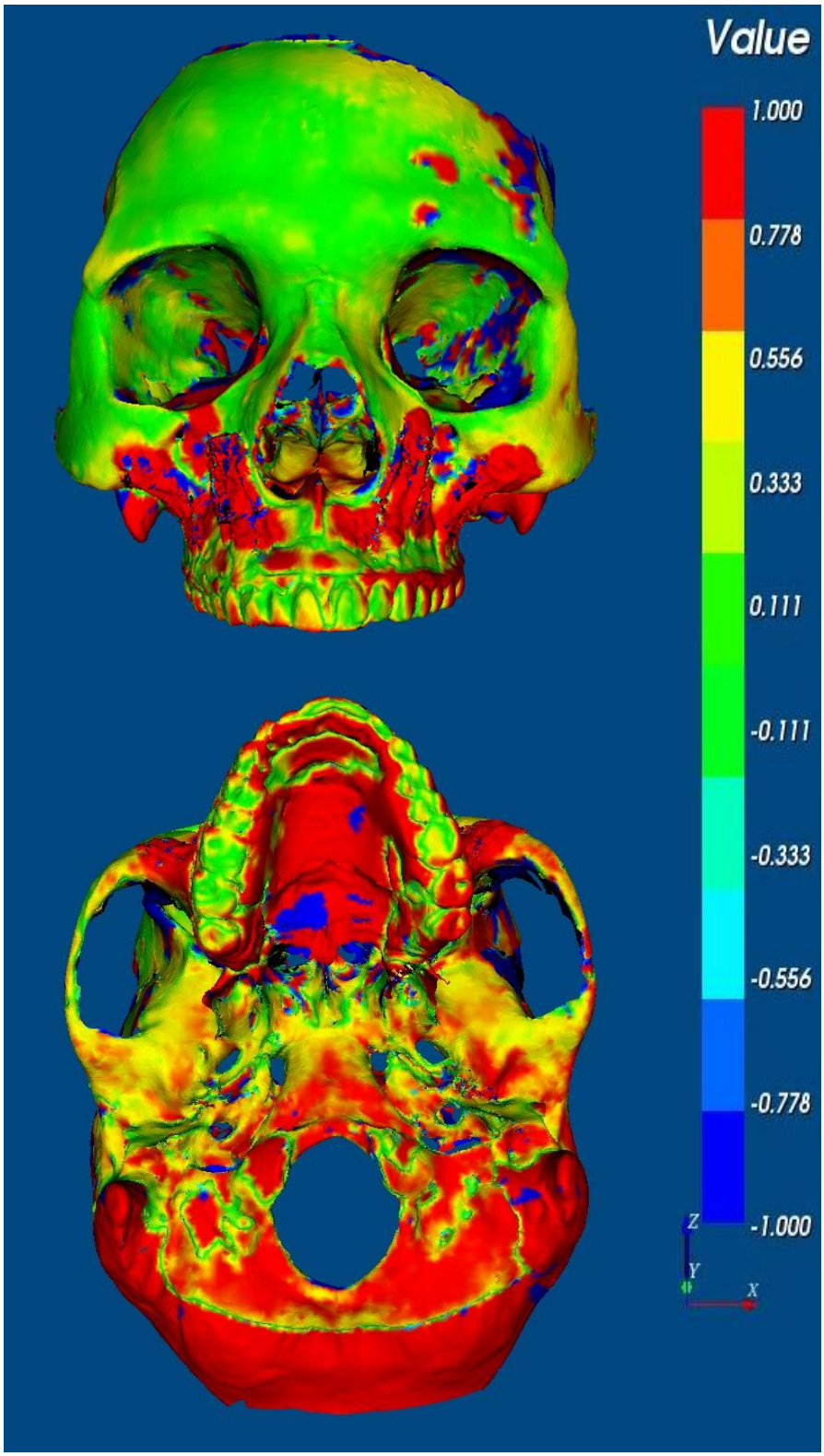

Figure 5.6 Human skull 6 mesh superimposed on the vault only of the 3D skull printed model with plaster teeth mesh using VRmesh. The distance between the meshes is indicated by the colour.

6

Discussion and Conclusions

6.1 Discussion

The aim of this project was to determine the accuracy with which the distorted dentition produced on a 3D printed skull model could be replaced using a novel method. The technique involved the replacement of the dental arch of a 3D printed skull model with a dental plaster cast taken from a direct impression of the human skulls' dentition. This would provide an alternative method to conventional orthognathic model planning prior to final orthognathic surgery wafer construction. At present orthognathic surgery planning relies on using a facebow registration to transfer the maxillary position relative to the base of the skull onto a semi-adjustable articulator. The inherent inaccuracies of the present system have been well documented (Walker *et al.*, 2008; Sharifi *et al.*, 2008; Ellis *et al.*, 1992; Pitchford *et al.*, 1991; Bailey and Nowlin, 1984; Stade *et al.*, 1982; Gonzalez and Kingery, 1968).

The distortion of the dentition as a result of the CBCT scanning is well known and is mainly due to beam hardening. The artefact occurs because the high density metal absorbs the lower energy photons while the higher energy photons pass through to the detectors which results in the beam becoming 'harder' and streaked (Barrett and Keat, 2005). In order to replace this distorted dentition, the degree of distortion needs to be calculated and known. The dentition of the 3D printed skull model has been shown to exhibit a degree of magnification that occurs firstly as a result of the CBCT scan but also possibly in association with the printing process. Comparing dental dimensions for the 3D printed skull model with those from the corresponding human skull showed a significant degree of magnification ranging from 0.5mm to 1.0mm. Unfortunately the degree of magnification was not uniform in all directions. This may have been due to the CBCT scanning process, due to the direction the model was printed or a combination of both. The scans were carried out in 0.4mm slice thicknesses and the model was printed in 1mm thick layers.

Depending on which way the model was printed the underlying print resolution would determine the accuracy of the final model.

6.2 Errors of the method

6.2.1 Dental Impressions

The first stage of the technique involved obtaining a replicate model of the upper human teeth using a silicone impression material to produce a negative copy and then dental stone was used to produce the positive cast. This was then used to produce a splint, which was constructed for transferring the plaster dentition onto the 3D printed skull model. A hard polyvinyl splint of 1mm thickness was made for the transfer of the plaster dentition onto the 3D printed skull model. The initial pilot study showed that the degree of magnification of the 3D printed skull dentition was approximately 1.0mm and therefore the 1.0mm splint would compensate.

By taking an impression of the 3D printed skull model dentition and placing the 1.0mm splint into the impression and then pouring plaster into the splint, to produce an accurate dentition, the magnification of the 3D printed model could be compensated.

To access the error at this stage, a comparison of the landmarked laser scanned data from the plaster dentition, obtained via the splint and from the landmarked natural skulls' dentition, could be made. The results showed that the mean error was 0.55mm. Therefore the process of producing a replicate dentition relied on the internal surface of the splint being 1.0mm thick. This assumed that the magnification error was uniformly 1.0mm across the surfaces of all the teeth. The results show that this is not the case but could vary from 0.3mm up to 1.5mm; unfortunately it would be difficult, if not impossible, to construct a non-uniform thickness splint.

6.2.2 3D printed skull models

As a result of this study it was discovered that the 3D printed skull model was larger than the respective human skull with an overall mean error of 0.42mm. However, for skull models used routinely in medicine this margin of error would be clinically acceptable.

The 3D printed skull models for this project were made from a non-robust gypsum powder material which proved to be brittle and fragile *(Figure 6.1).* Due to the skulls' material fabric, any abrasion of the skull could lead to a loss of dimensional accuracy therefore great care had to be taken when carrying out the transfer process. An alternative method of model construction was to use either a Stereolithographic model or fused deposition modelling. Stereolithographic models are made by using a bath of photosensitive resin and an ultra-violet laser for curing the resin however; this is a costly process and is not likely to be used routinely in orthognathic surgery planning *(Figure 6.2).* Fused deposition models are made from an Acrylonitrile Butadiene Styrene (A.B.S.) material; this is a thermoplastic material which is extruded from a fine nozzle not unlike an electric glue gun. This technique has been widely used for building 3D skull models because of its good dimensional stability, rigidity and relatively low cost *(Figure 6.3).* The use of a robust 3D skull model could enhance the quality of the repositioning of the maxillary process after the dentition has been replaced and as a result the locating plates and screws would probably be more accurately sited without any abrasion to the 3D printed skull models surface or screw holes.

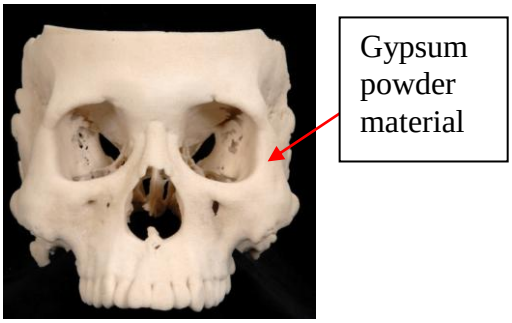

Figure 6.1 Gypsum powder model.

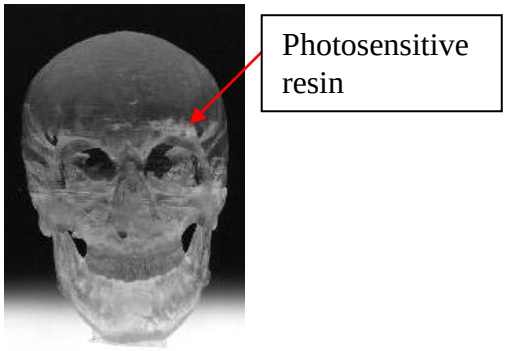

Figure 6.2 Stereolithography model.

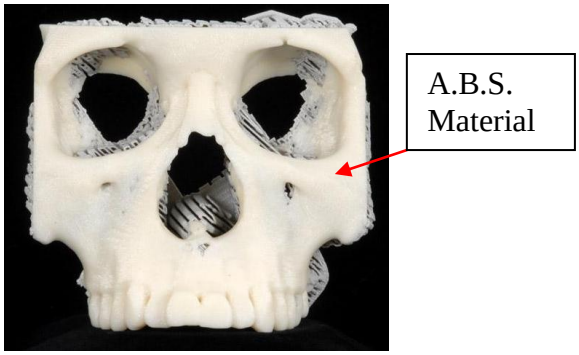

Figure 6.3 Fused deposition model.

6.2.3 Locating plates and screws

The locating plates were positioned and removed in sequence; this was carried out in order to allow correct alignment of the dentoalveolar maxillary process, when reattaching it to the 3D printed skull model after replacement of the incorrect dentition had taken place. Although the locating plates were placed and removed in sequence, the self tapping surgical screws were not removed or replaced in sequence. This highlighted a margin for error when replacing the maxillary process to the 3D printed skull model as the alignment could be marginally different when it was re-attached.

A better solution would be to remove and replace the surgical screws in sequence in a similar manner as for the locating plates. Implementing this procedure with the self tapping surgical screws would help to enhance the accuracy of the reattachment of the

dentoalveolar maxillary process with the replaced dentition. The use of a torque wrench to measure the amount of pressure applied to the screw might also be an advantage.

6.2.4 The transfer jig

The transfer jig was a device which aided transfer of the dentition onto the 3D printed skull model. It had three fixed vertical height parallel columns, which ensured that when the dentition was transferred from the 3D printed skull models' maxillary process and replaced with the plaster dentition, the vertical dimension was maintained. A potential improvement for the transfer technique would be the use of a more rigid, less compressive impression material rather than silicone putty. As the transfer jig is closed, a force is applied which could result in the splint being compressed into the flexible silicone impression material causing the splint to alter. In addition to this is the inherent flexibility of the splint and the contraction and expansion of the plaster when it is poured onto its interior surface could cause further inaccuracies.

A possible solution would be to secure the splint into position in the silicone impression using adhesive. This would ensure the splint remains in position but this solution could also prove to be problematic as it might not deal with the compression forces when the transfer jig is closed. The flexibility of the splint could be reduced by leaving the splint on the original model it is fabricated on, the splint could be trimmed with the original model in situ, thus omitting any further mixing of dental plaster; however there would still be the issue of flexibility of the impression material. Using less flexible materials may benefit the method of dentition transfer.

6.3 Measuring the accuracy of plaster dentition replacement

In order to investigate the true level of accuracy for the replacement of the plaster dentition in relation to the human skull, laser scans were taken of both the 3D printed skull models with plaster dentition and the human skulls. Laser scanning was favoured over a co-ordinate measuring machine to indicate the level of accuracy obtained because co-ordinate measuring involves a touch probe that has to be physically guided to certain selected points on the skull to register x, y and z co-ordinate landmarks.

Laser scanning the images was deemed to be more useful since x, y and z co-ordinates can be obtained and in addition a 3D topographical image can also be generated. The image is made up of millions of points either in the form of a point cloud or a polygonal mesh. The use of a mesh effectively aligns millions of individual points; the mesh can be landmarked and aligned using a mesh editing CAD/CAM software – VRmesh. Co-ordinate landmark points were chosen on the images that were recognisable on both human skulls and the 3D printed skulls models in order to superimpose the images. This software programme was designed to use a rigid registration based on corresponding landmarks and an iterative closest point (I.C.P.) algorithm for mesh alignment. This is where two similar shapes are aligned and superimposed over each other to the best possible fit. The distance between the meshes indicates the “closeness” of fit. Additionally VRmesh provides a colour indication of the levels of accuracy obtained.

6.4 Results

The mean dentition placement error was 0.19mm with a mean placement error for the skull vault of 0.11mm. However, the mean mapping and digitisation error was 0.55 mm for the dentition and 0.72mm for the vault. These results suggest that errors in the mapping and

the digitisation of the landmark points are much greater than the errors of the dentition placement technique. Therefore if digitisation and mapping of the landmarks could be improved then this should have a significant effect on the precision of this technique. With the present levels of accuracy preliminary studies have shown that this replacement technique could be clinically acceptable. Future plans should include repeating and analysing the digitisation using more accurate landmark points and carrying out an operator error study of dental arch placement using different operators.

6.5 Future developments

This preliminary research has shown that it has been possible to replace the dentition from a 3D skull model which would allow the skull to be used for the pre-planning of orthognathic surgical cases. However, the level of accuracy obtained would need to be measured against the accuracy of current techniques involving facebows and articulator systems to provide verification that 3D skull models were a more effective means for carrying out complex orthognathic surgery cases.

The sample size used for this project was relatively small and it was performed on human skulls. Further projects involving patients, which included clinical cases of varying complexity, would be required to investigate the benefits obtained comparing this with current methods for pre-surgical orthognathic planning. The planning of mandibular asymmetric surgical cases is already being carried out in this way to good effect. Printed skull models are likely to have great advantages over current methods of planning the correction of asymmetry cases. For example, the ability to measure the extent of a condylar shave required and visualise its effect on the surrounding skeletal areas prior to entering the operating theatre, would be very helpful for this type of deformity.

With the evolvement of this technology the surgeon is offered more information when repositioning the jaws in relation to the skeletal profile than can be obtained from dental articulators that operate only on the dental arch. Technology needs to develop and improve with enhancements in the conversion software and faster applications would be essential. This would lead the way for virtual orthognathic planning on a visual monitor (Swennan *et al.*, 2009) with the ability to produce a computer milled surgical wafer to use as a template for repositioning the jaws in theatre. However, there are still benefits from a hand held 3D skull model which allow surgeons to have a tactile approach prior to surgical procedures, which might eliminate surprises in theatre. Additional benefits would be the saving of theatre time, allowing bone plates to be shaped prior to the operation and templates to be created for bone grafts. The 3D skull models would also be a visual educational input for training clinical staff and would be a help to explaining to patients the procedures that were to be performed.

At present the cost of producing a 3D skull model is expensive when compared to the techniques currently available; they also rely on experienced personnel to operate the necessary equipment for their production. It should also be noted that the cost of this technology is reducing, making it more affordable for larger specialist units to purchase. Smaller units and departments could liaise with larger ones to make use of this technology more cost effectively and this would add another dimension to improving the accuracy of surgery. Continuing research has to be undertaken at various stages of this process in order to offer the appropriate levels of accuracy for pre-planning orthognathic surgery.

The current level of accuracy for replacing the maxillary dentition on the 6 skull models has been encouraging; however, since this study was carried out, the technique for replacement of the dentition has been enhanced, but this has not yet been proven. Further

study is needed to prove that these enhancement techniques will in fact led to improved accuracy.

Maxilim conversion software was used in this study to convert the DICOM files into an STL format. However, there are other conversion software packages available and research is required to compare the accuracy of the skull models produced using these different programmes. It has also been stated in this study that there are a number of methods for producing 3D skull models and research work is needed to prove which materials and production methods would best suit the requirements for orthognathic surgery planning.

Now that an accurate dentition can be satisfactorily located on the 3D printed skull model, the next step is to investigate how these models can be put to best use in orthognathic surgery planning. In order to do this a platform for mounting the 3D printed skull model requires to be designed and fabricated. The platform would be essential to hold the skull securely, whilst allowing movement of both dental arches with appropriate measuring gauges registering vertical, horizontal and rotational movements of both dentitions. A suitable prototype is presently being constructed but further development in this area is required.

6.6 CONCLUSION

An accurate and valid method has been described for the transfer of the dentition onto a 3D printed skull model. It also transfers a portion of the alveolus and shows the changed position of the bone structures at the time of osteotomy and it allows preplanning of the bone graft required with inferior maxillary repositioning. The precise position is enhanced by the ability to shape the plates and position screws prior to surgery and this should shorten theatre time.

7

References

References

ALBERTI, C., 1979. Three-dimensional CT and structure models. *Br J Radiology,* **53**, 261-262.

BAILEY, J.O.,JR and NOWLIN, T.P., 1984. Evaluation of the third point of reference for mounting maxillary casts on the Hanau articulator. *Journal of Prosthetic Dentistry,* **51**(2), 199-201.

BAMBER, M.A., HARRIS, M. and NATCHER, C., 2001. A validation of two orthognathic model surgery techniques. *J Orthod,* **28**, 135-142.

BARKER, T.M., EARWAKER W.J.S., LISLE, D.A., 1993. Integration of 3-D Medical Imaging and Rapid Prototyping to Create Stereolithographic Models. *Aust. Phys. Eng.Sci,* **16**(2), 79-85.

BARRETT, J.F., KEAT, N., 2004. Artifacts in CT: Recognition and Avoidance. *RadioGraphics,* **24**, 1679-1691.

CHOI, J.Y., CHOI, J.H., KIM, N.K., KIM, Y., LEE, J.K., KIM, M.K., LEE, J.H. and KIM, M.J., 2002. Analysis of errors in medical rapid prototyping models. *International Journal of Oral & Maxillofacial Surgery,* **31**(1), 23-32.

DOWNS W. B., 1956. Analysis of the Dentofacial Profile. *Angle Orthod,* **26**, 192-212.

DRYDEN, I. L., MARDIA, K. V., 1998. Statistical shape analysis, Chichester: Wiley.

ELLIS III, E., THARANON, W. and GAMBRELL, K., 1992. Accuracy of face-bow transfer: Effect on surgical prediction and postsurgical result. *Journal of Oral and Maxillofacial Surgery,* **50**(6), 562-567.

FERRARIO, V.F., SFORZA, C., SERRAO, G. and SCHMITZ, J.H., 2002. Three dimentional assessment of the reliability of a postural face-bow transfer. *Journal of Prosthetic Dentistry,* **87**, 210-215.

FUHRMANN, R.A., FROHBERG, U. and DIEDRICH, P.R., 1994. Treatment prediction with three-dimensional computer tomographic skull models. *American Journal of Orthodontics & Dentofacial Orthopedics,* **106**(2), 156-160.

GATENO, J., FORREST, K.K., CAMP, B., 2001. A comparison of 3 methods of face-bow transfer recording: Implications for orthognathic surgery. *J Oral &Maxillofac Surg,* **59**, 635-640

GOLD, B.R. and SETCHELL, D.J., 1983. An investigation of reproductability of face bow transfer. *J Oral Rehab,* **10**, 495-503.

GONZALEZ, J.B. and KINGERY, R.H., 1968. Evaluation of planes of reference for orientating maxillary casts on articulators. *J Am Dent Assoc,* **76**, 329-336

.

GUYURON, B. and ROSS, R.J., 1989. Computer-generated model surgery. An exacting approach to complex craniomaxillofacial disharmonies.*The Journal of Cranio-Maxillo-Facial Surgery,* **17**(3), 101-104.

HIEU, L.C., ZLATOV, N., VANDER SLOTEN, J., BOHEZ, E., KHANH, L., BINH, P.H., ORIS, P., TOSHEV, Y., 2005. Medical rapid prototyping applications and methods, *Assembly Automation,* **25,** (4), 284 - 292

KARCHER, H., 1992. Three-dimensional craniofacial surgery: Transfer from a three-dimensional model (Endoplan) to clinical surgery: A new technique (Graz). *Journal of Cranio-Maxillo-Facial Surgery,* **20**(3), 125-131.

KLEIN, H.M., SCHNEIDER, W., ALZEN, G., VOY, E.D., GUNTHER, R.W., 1992. Pediatric craniofacial surgery: comparison of milling and Stereolithography for 3-D model manufacturing. *Pediatr Radiol,* **22**,458-460.

KRAGSKOV, J., SINDET-PEDERSEN, S., GYLDENSTED, C., JENSEN, K.L., 1996. A comparison of three-dimensional computed tomography scans ad stereolithographic models for evaluation of craniofacial anomalies. *J Oral & Maxillofac Surg,* **54**, 402-411.

LAMBRECHT, J.T., BRIX, F., 1990. Individual skull model fabrication for crainiofacial surgery. Cleft Palate Journal, **20**, 382-386

LILL, W., SOLAR, P., ULM, C., WATZEK, G., BLAHOUT, R. AND MATEJKA, M., 1992. Reproducibility of three dimensional CT-assisted model production in the maxillofacial area. *Br J Oral Maxillofac Surg,* **30**, 233-236.

MAVILI, M.E., CANTER, H.I., SAGLAM-AYDINATAY, B., KAMACI, S. and KOCADERELI, I., 2007. Use of three-dimensional medical modeling methods for precise planning of orthognathic surgery. *The Journal of Craniofacial Surgery,* **18**(4), 740-747.

MOOREES C.F.A, K.M.R., 1958. Natural head position, a basic consideration in the interpretation of cephalometric radiographs. *Am J Phys Anthropol,* **16**, 213-234.

PETZOLD, R., ZEILHOFER, H.F., KALENDER, W.A., 1999. Rapid prototyping technology in medicine - basics and applications. *Computerized Medical Imaging and Graphics.* **23**, 277-284.

PHAM, D.T. and GAULT, R.S., 1998. A comparison of rapid prototyping technologies. *The International Journal of Mechine Tools & Manufacture,* **38**, 1257-1287.

PITCHFORD, J.H., 1991. RE-evaluation of the axis orbital plane and the use of orbitale in the facebow transfer record. *J.Prosthet.Dent.,* **66**, 349-355.

ROHLF, F.J. 1999 Shape Statistics: Procrustes Superimpositions and Tangent Spaces. *Journal of Classification,* **16**, 197-223.

SAILER, H.F., HAERS, C.P., ZOLLIKOFER, C.P.E., WARNKE, T., CARLS, F.R. and STUCKI, P., 1998. The value of stereolithographic models for preoperative diagnosis of crainiofacial deformaties and planning of surgical corrections. *Int.J.Oral Maxillofac.Surg.,* **27**, 327-333.

SANTLER, G., 1998. The Graz hemisphere splint: a new precise, non-invasive method of replacing the dental arch of 3D-models by plaster models. *Journal of Cranio-Maxillo-Facial Surgery,* **26**(3), 169-173.

SHARIFI, A., JONES, R., AYOUB, A., MOOS, K., WALKER, F., KHAMBAY, B. and MCHUGH, S., 2008. How accurate is model planning for orthognathic surgery? *International Journal of Oral and Maxillofacial Surgery,* **37**(12), 1089-1093.

STADE, E.H., HANSON, J.G. and BAKER, C.L., 1982. Esthetic considerations in the use of face-bows. *Journal of Prosthetic Dentistry,* **48**(3), 253-256.

SWENNEN, G.R.J., BARTH, E., EULZER, C. and SCHUTYSER, F., 2007. The use of a new 3D splint and double CT scan procedure to obtain an accurate anatomic virtual augmented model of the skull. *International Journal of Oral & Maxillofacial Surgery,* **36**(2), 146-152.

SWENNEN, G.R.J., MOMMAERTS, M.Y., ABELOOS, J., De CLERCQ, C., LAMORAL, P., NEYT, N., CASSELMAN, J., SCHUTYSER, F., 2009. A cone-beam CT based technique to augment the 3D virtual skull model with a detailed dental surface *International Journal of Oral and Maxillofacial Surgery,* **38**, *Issue (1), 48-57.*

TERAI, H., SHIMAHARA, M., SAKINAKA, Y. and TAJIMA, S., 1999. Accuracy of integration of dental casts in three-dimensional models. *Journal of Oral & Maxillofacial Surgery*, **57**(6), 662-665.

WALKER, F., AYOUB, A.F., MOOS, K.F. and BARBENEL, J., 2008. Face bow and articulator for planning orthognathic surgery: 1 face bow. *British Journal of Oral & Maxillofacial Surgery*, **46**(7), 567-572.

WALKER, F., AYOUB, A.F., MOOS, K.F. and BARBENEL, J., 2008. Face bow and articulator for planning orthognathic surgery: 2 articulator. *British Journal of Oral & Maxillofacial Surgery*, **46**(7), 573-578.

WINDER, J. and BIBB, R., 2005. Medical rapid prototyping technologies: state of the art and current limitations for application in oral and maxillofacial surgery. *Journal of Oral & Maxillofacial Surgery*, **63**(7), 1006-1015.

Glossary

Articulator.	A mechanical device to which plaster casts of the upper and lower dental arches are attached and which artificially reproduces recorded positions of the mandible in relation to the maxilla.
Facebow.	An instrument used to record the transverse horizontal axis (hinge axis) of the mandible and relating this recording to the maxilla to facilitate. anatomical mounting of the maxillary cast to the articulator.
Frankfort horizontal plane.	A plane passing through the left orbitale (most inferior point of the orbit) and the highest point of each external auditory meatus.
Axis orbital plane.	An imaginary line joining orbitale and the axis of mandibular rotation.
Skull model.	Replica of the human skull constructed from volumeric CT scan data.
3D	Three dimensional.
MRI	Magnetic Resonance Imaging.
CBCT	Cone beam computed tomography scan.
DICOM	Digital image communications in medicine.
STL	Single tessellation language.